Performance Analysis of Dye Sensitized Solar Cell based on ZnO Compact Layer and TiO_2 Photoanode

Submission of Thesis to the

Department of Electrical and Electronic Engineering (EEE)

Of

BRAC University

to ensure the partial fulfillment as a requirement for complementation

Of Bachelor of Science degree in

Electrical and Electronic Engineering.

Abdur Rahman

Md. Ashik Mahmud

Md. Inzamamul Haque

Declaration

We, the participators of Thesis entitled "Performance Analysis of Dye Sensitized Solar Cell based on ZnO Compact Layer and TiO_2 Photoanode" under the Department of Electrical and Electronic Engineering (EEE) of BRAC University is being submitted to ensure complementation of degree of Bachelor of Science in Electrical and Electronic Engineering. We hereby disclose the fact that the submitted thesis work is completely our core work and also declare its originality. We strongly confirm that the work has not been published anywhere else for any other purposes.

Date: 4th September 2018

Dr. Md. Belal Hossain Bhuian
Thesis Supervisor

Abdur Rahman
Student ID: 13121011

Md. Ashik Mahmud
Student ID: 12221020

Md. Injamamul Haque
Student ID: 13121124

Acknowledgement

We would like to express our gratitude and love to our honorable faculty, supervisor, Dr. Mohammad Belal Hossain Bhuian, Assoc. Prof. Department of Electrical and Electronic Engineering (EEE), BRAC University for his tremendous support, assistance and continuous supervision along with constructive feedbacks during the period of this thesis work. His guidance has enabled us to develop our core work and concepts needed for Thesis. It would not be feasible to complete the thesis work without his guidelines and assistance. We are also grateful to the Department of Electrical and Electronic Engineering (EEE), School of Engineering and Computer Science, BRAC University for providing us with the necessary facilities.

Abstract

Harnessing solar energy as an alternative solution to power production. Power can be produced through burning fossil fuels. To gain optimum benefit through solar energy is an extreme challenge for scientists and researchers nowadays. Solar power generation is consistently improving through the decades and third generation dye sensitized solar cell can play an important role as a solution. Dye sensitized solar cell approaches to high efficient thin film technology. Efficiency can be increased by adding more cells of different band gap to a cell stack in Tandem cell. In this ongoing study, a double layer structured dye sensitized solar cell has analyzed where ZnO and TiO_2 composited photoanode were prepared on FTO. The Photovoltaic characteristics, I-V & J-V curve were evaluated for different thickness, absorption coefficient and wavelength. DSSC solar cell characterization techniques such as current-voltage and spectral response measurements were analyzed to evaluate the cell performance.

CONTENTS

Chapter 3: Study of Thickness Effect on Dye Sensitized Solar Cell

Chapter 4: Optical Transmission Spectrum Analysis

Chapter 5: JV Characteristics and Performance Analysis

List of Figures

Chapter 1

Introduction to Dye Sensitized Solar Cell (DSSC)

1.1 Motivation

Harnessing solar energy as an alternative solution to power production. Power can be produced through burning fossil fuels. To gain optimum benefit through solar energy is an extreme challenge for scientists and researchers nowadays. Over last few years, significant improvements have been noticed in power production through renewable sources of energy. Increasing demand for power and energy globally and rising of sea level water as a result of global warming are most alarming situations for the present world. Burning fossil fuels is considered as a major environmental threat due to substantial contribution to greenhouse gases as a result of increasing global temperature. Cost efficient, environmentally clean and sustainability are main factors that are playing vital role in terms of energy consumption as well as production and scientists, researchers are continuously trying to figure out such a renewable source of energy nowadays.

Dye Sensitized Solar Cell is a third generation solar cell invented by Michael Grätzel [1, 7]. It is one of the promising methods of harnessing solar energy, as the dyes are not needed to be highly purified and cost effective. Through the efficiency of Dye Sensitized Solar Cell are comparatively less than Silicon based solar cell, still it has drawn great attractions to scientists and researchers as dyes can be modified and multi-layer Nano structured photoanode can be used to gain more efficiency and stability. Typically, photoanodes, for example: TiO_2, ZnO, SnO_2, NB_2O_5, which are considered wide band gap semiconductors.

Basically in Dye Sensitized Solar Cell (DSSC), electron and hole pairing through recombination is considered as decreased performance. On the other hand, high electron mobility is needed for improved photovoltaic performance of DSSC. Using single layer photoanode structured semiconductor in the preparation of DSSC is less efficient compared to multiple layer structured

DSSC. Single layer structured photoanode consisting of semiconductors having low electron mobility are not able to improve the photovoltaic performance up to mark.

To overcome this problem one of the most effective solutions can be using compact layer in the DSSC preparation of cell structure where two or more photoanodes (multiple) layer deposition has proved to be much efficient and significant particularly. Therefore, in this performance evaluation of DSSC, we considered TiO_2 photoanode and ZnO Compact layer based DSSC that was investigated for further analysis.

In this thesis, we have divided the work in particulars chapters where **Chapter 1** has elaborate discussion of solar cell, generation based solar cell, solar cell circuit model and brief study of Dye Sensitized Solar Cell (DSSC) with compact layer and Oxide composite DSSC.

In Chapter 2, Theoretical model of DSSC has been described. I-V characteristics have been figured out in this chapter through analytical equations derivations along with parameters value extraction from reference sources and a MATLAB code was being developed to simulate I-V properties of TiO_2, ZnO and combination of both photoanodes together. The performance of the photoanodes was evaluated separately and through proper combination.

In Chapter 3, effect of thickness in Photocurrent Density vs. Voltage (J-V) has been analyzed for TiO_2, ZnO and for both combinations through simulation. Calculation of internal parameter of DSSC, results and discussion were included finally of the chapter.

Optical Transmission Spectrum has been analyzed in **Chapter 4** where brief study of TiO_2 and ZnO properties were identified. Effect of ZnO thin film on Glass (N-BK7) substrate has been calculated and shown in figure. On ther hand, TiO_2 effect on Fluorine doped Tin Oxide (FTO) Glass has been analyzed along with derived graphical figure from simulation. This chapter

focused on simulation of Absorbance vs. Wavelength for TiO_2 and ZnO. Our main concern was to figure out the absorbance for particular wavelength and materials behavior towards optical spectrum.

MATLAB simulation code was developed through analytical equations derivation and parameters were being extracted for further calculation. Results of simulation were discussed elaborately along with comparative analysis in this chapter.

In Chapter 5, the effect of extracted Absorption Coefficient on J-V characteristics has been analyzed on TiO_2, ZnO and typically on both materials. Results of comparative simulation have been discussed. Analysis and discussion took place at the end of this chapter.

Chapter 6 focuses challenges that we faced during our thesis work, difficulties to find out the parametric equations values, overcoming problems and briefly discussed further scopes of our work.

1.2 Introduction

Energy has become one of the most important parts of this modern time of technology. Every sector of technologies is depending over energy source. With the increase of world population, the demand of energy is expected to be double in next 1.5 decade as the consumption of power is increasing day by day. Around 80% of world energy is supplied by Fossil fuel like natural gas, coal and oil. The amount of natural resources will not increase with the demand. Nuclear energy production system is costly and dangerous; many countries have shut down their Nuclear Power Plant because of its complexity. Therefore, we have to start giving more importance focusing on renewable energy sources. Solar energy can play an important role as a source of renewable energy because they are cheaper, generates no greenhouse gas or any other chemical by-products like the burning of fossil fuel. For solar energy, the mining of raw materials like oil or coal are not needed, materials which have to be extracted, refined and then transported to a power plant. Every year from sunlight, we receive about 3 x 10^{24} joule energy. In the form of sunlight to the earth's surface, this is more than the consumption rate of energy of the world per year.

1.3 Solar Cell

Solar energy produces power through solar panel. Solar panels are made of solar cell or photovoltaic cells (PV) which contain material that responds to solar radiation. Solar cell absorbs the solar radiation and converts it into electrical energy from photon energy of solar radiation through solar panel. Solar cell using sun for its source of energy and sun is ultimate energy provider, increasing the use of solar cell will be more efficient economically as solar cell does not have negative impact over environment. There are many advantage of solar cell; few of them are highlighted below.

- Renewable energy
- Environmentally friendly
- Low cost
- Long-term stability

In solar cell, one forward biased diode is connected with current source in parallel. Then one series resistance and shunt resistance added in parallel. Series resistance, Rs in a solar cell is the result of contact resistance and charge transfer resistance in the semiconductor material [2]. Series resistance reduces the fill factor affecting the maximum power output, while excessively high value of Rs (series resistance) can also decrease the short-circuit current. On the other hand, low shunt resistance provides an alternate current path for the photo-generated current causing significant power loss. The effect of low shunt resistance is decreased fill factor and lower V_{oc} affecting the maximum power output.

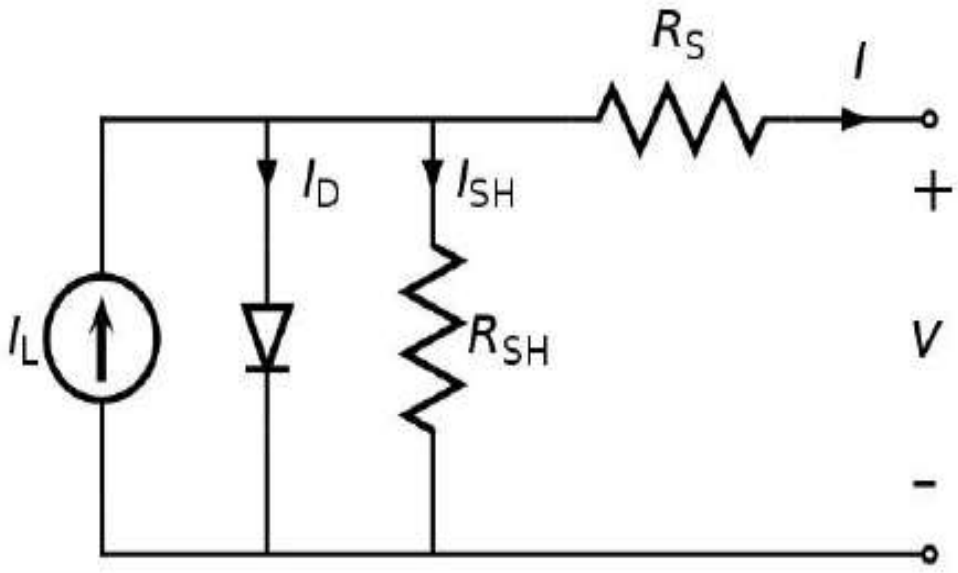

Fig 1.1: Solar Cell Equivalent Circuit [2]

1.4 Different Generations of Photovoltaic Cell

There are three generation of photovoltaic cell (PV cell). In first generation, more importance has been given on efficiency. Most of the first generation solar cells are expensive though they are more efficient. They are mainly based on silicon wafer. Photo generated electron hole pair is separated and collected through p-n junction of a doped semiconductor. Most of the first generation solar cells are monocrystalline solar module where light induced degradation (LID) system is widely popular. Most of the solar panels in market are based on first generation solar cell. The efficiency of these solar cells is around 15-20% [3].

The second-generation photovoltaic cells are usually based on amorphous silicon and CdTe. The performance of these solar cells is around 10-15%. Since the second-generation solar cell keep away from the use of silicon wafers and have a decrease fabric consumption it has been possible to limit production expense of these solar cells compared to the first generation [3]. The second generation can be produced in some flexible temperature in vacuum method but in this process, the requirement temperature is excessive which increase the manufacturing cost.

In third generation solar cell, one of the major benefits is that it does not have any relation with Shockley-Queisser theoretical limit, which was a drawback for first and second-generation solar cell [3]. There are mainly five types of third generation solar cell, CZTS, Dye sensitized solar cell, Quantum dot solar cell, Perovskite solar cell and Organic solar cell [33].

1.5 Dye Sensitized Solar Cell

Dye sensitized solar cell is one of the third generation solar cell. The photovoltaic effect of Dye sensitized solar cell was first demonstrated by Michael Grätzel and O'Regan in 1991 [4] but the production of electricity for organic dyes had started in l960. Grätzel bought a revolutionary change in Dye sensitized solar cell. Dye sensitized solar cell is a relatively new photovoltaic device which have been extensively investigated and received tremendous attention because of their affordable cost and non-environmental polluted process. Dye sensitized solar cell often said

as artificial photosynthesis because of its mimic nature of absorbing sunlight. Dye sensitized solar cell produce electricity when it is sensitized by light. The dye of DSSC response into sunlight and collect photon to use their energy, then the energy is used for excitation of electron. After that, the dye injects those excited electrons in Titanium Dioxide, which later carried away into a crystal of titanium dioxide where the electrons are conducted [1]. To close the circuit, an electrolyte is added. Then the movement of inside electron created electricity.

1.6 Advantage of Dye Sensitized Solar Cell

If we compare the power conversion efficiency of DSSC to other inorganic 1st and 2nd generation solar cells, we will see the efficiency conversion rate is lower than the other solar cell but it has few advantages over them. In the normal operating temperature range of 25–65ºC, the efficiency of DSSC is less dependent on temperature. In diffuse sunlight or cloudy conditions, the efficiency of Si based solar cell is around 20% [33]. On the other hand, DSSC have better efficiency in these conditions than polycrystalline Si solar cell. Performance is less sensitive to the incident angle of the light radiation; hence, a solar tracking mechanism is less necessary. Although a very commercial production of DSC is still not available, it can be expected that it is cheaper than all other thin film device. Only low cost and profusely available materials are needed. Unlike amorphous silicon, CdTe or CIGS cells, DSSC can be more efficient by avoiding all the expensive and energy-demanding high vacuum as well as materials distillation steps [5].

1.7 Compact Layer & Oxide Composite DSSC

In DSSC, the recombination of EHP usually decreases the photovoltaic performance significantly. Using a compact layer is a good solution to increase Photovoltaic performance. The compact layer is usually fabricated Fluorine doped Tin Oxide. Researchers are trying to implement anti-reflective coating, which is based on silicon on p-n junction solar cell to increase transmittance [7]. TCO prevent back electron transfer occurring in the interface between

transparent conductive oxide layer and electrolyte. The thickness of the compact layer has influence in open circuit voltage, which is connected with efficiency enhancement of dye-sensitized solar cell. There are many oxide layer has been tested as compact layer like TiO_2, MgO, In_2O_3, Nb_2O_5 [4].

After evaluating all of these compact layer performance, it has been seen that TiO_2 compact layer can improve the adherence to FTO surface but TiO_2 layer cannot improve the open circuit voltage because it got similar conduction band energy of TiO_2 absorption layer. ZnO layer can be a used as a solution because ZnO compact layer can create a barrier between FTO and TiO_2. The binding energy for ZnO is high as well as it is transparent in the visible light. The resistivity of ZnO is low. The ZnO with different of morphologies have been created by the use of different method such as hydrothermal synthesis [6]. As the negative conduction band range is higher for ZnO comparing to TiO_2, it will restrain the recombination and improve the open circuit voltage at the same time. The transfer rate of charge is also higher for ZnO [5].

In our analysis, we have observed a double layer structure for photoanode of Dye sensitized solar cell. ZnO compact layer is used as first layer. The second layer is TiO_2 layer. Then we have studied the performance of ZnO compact layer and TiO_2 layer for different thickness, absorbance, wavelength and transmittance individually and together.

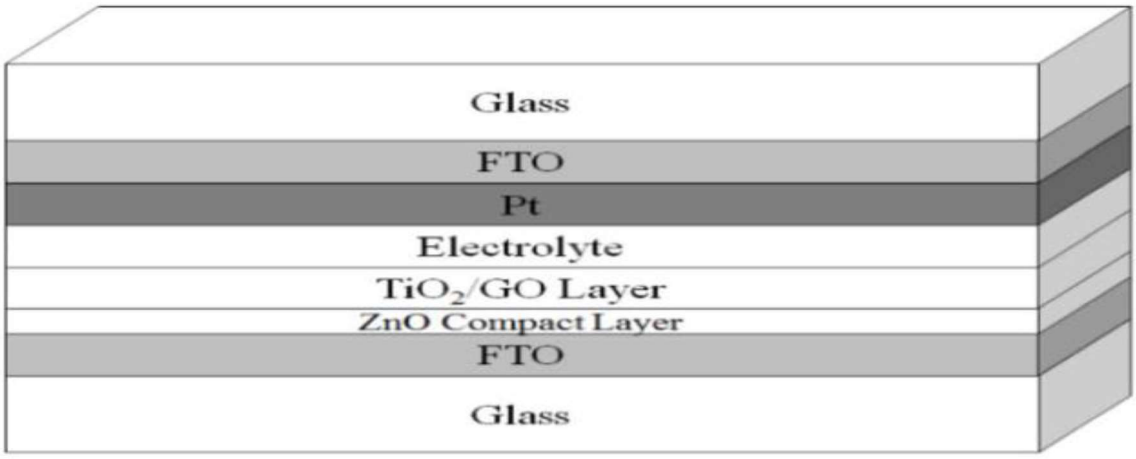

Fig 1.2: The structure of the DSSC including ZnO compact layer and TiO_2 layer [4]

1.8 Operation Principle of DSSC

At the center of the system is a mesoporous oxide layer composed of nanometer particle deposited by melting which form bridges between two particles to allow electronic conduction. In this case, TiO_2 is mostly used. However, ZnO is also investigated as an alternative band gap oxide. Figure 1.2, shows the structure of DSSC for compact layer in this study.

The Dye sensitized solar cell usually contains five components [7]:

- A mechanical support coated with transparent Conductive Oxides
- The semiconductor film, usually TiO_2, (ZnO and Nb_2O_5 also used).
- A sensitizer which is adsorbed into the surface of the semiconductor material
- An electrolyte containing a redox mediator. (Usually used for neurotransmitter)
- A counter electrode capable of regenerating the redox mediator

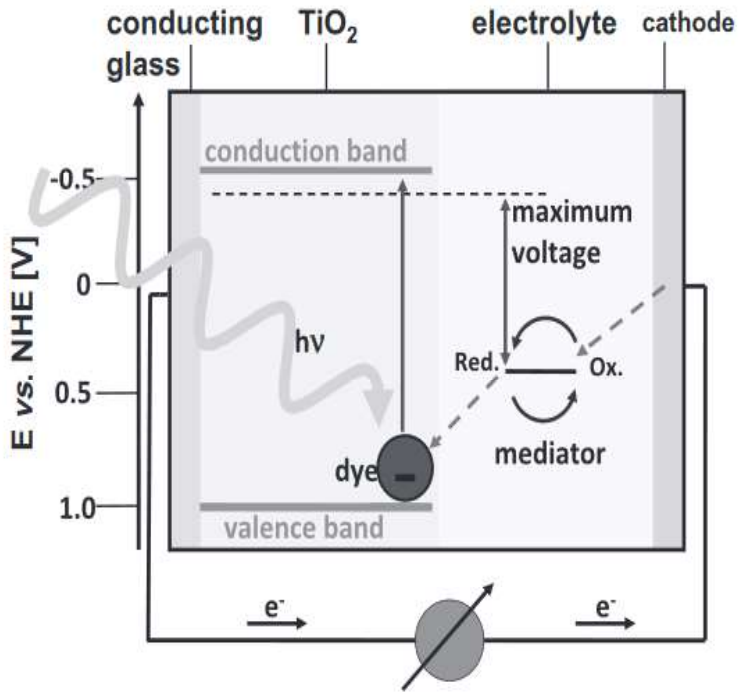

Fig 1.3: Operating principles and energy level diagram of dye-sensitized solar cell [7]

The nanocrystalline film of DSSC is a monolayer which is a part of dye that is used for charge transfer by donating electron from the electrolyte, the original state of the dye is subsequently restored which is usually an organic solvent containing redox system for example, iodide and tri-iodide [7]. The regeneration of the sensitizer by iodide intercepts the recapture of the conduction band electron by the oxidized dye. The iodide is recreated at the counter electrode by the reduction of tri-iodide to complete the circuit by electron migration through the external load. The voltage generated under illumination corresponds to the difference between the Fermi level of the electron in the solid and the redox potential of the electrolyte. After all the process, the device generates electric power from light without suffering any permanent chemical transformation [7]. The Dye Sensitized Solar Cell (DSSC) uses the same basic principle as plant photosynthesis to generate electricity from sunlight. Each plant leaf in DSSC is photo chemical cell, which converts solar energy into biological material. The DSSC (a characteristic structure is shown in Fig. 1.4) is the only photovoltaic device that exploits dispersed mediums for light absorption/carrier generation (dye) and carrier transport (TiO_2 nano-particles).

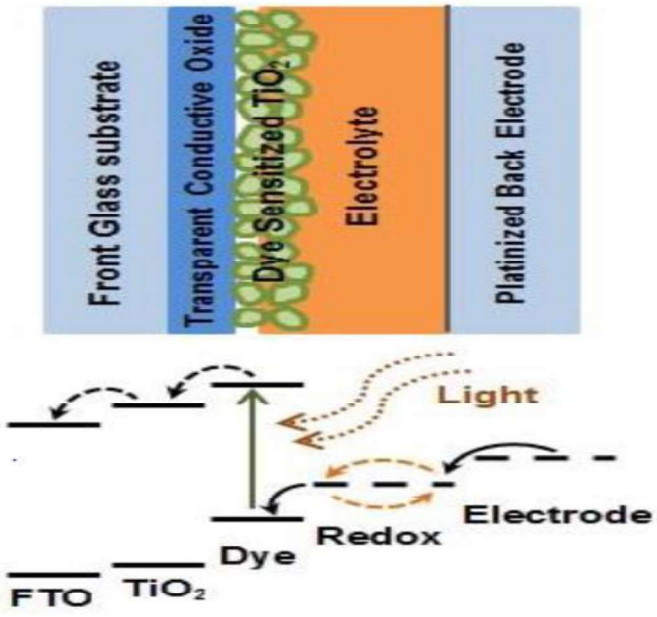

Fig 1.4: Band diagram of Dye Sensitized Solar Cell. [7]

First the light is absorbed by a sensitizer dye molecule, then it passes through an electronic state where it changes from ground (S) to the excited state (S*). The lifetime of the excitation states is usually in nanoseconds. The dye molecules which are sensitizing are adsorbed on the surface of a wide band gap semiconductor (usually TiO_2). On the basis of absorption of a photon (excitation), the dye gains the ability to transfer an electron to the conduction band of the semiconductor [1].

The nanoparticles for the internal electric field causes the electron extraction and the dye becomes oxidized (S+). To make the electron injection more efficient the lowest unoccupied molecular orbital of the dye has to be about 0.3 eV above the TiO_2 conduction band. The nonporous TiO_2 film consists of spherical anatase particles of diameter ~20 nm [1]. The presence of oxygen vacancies in the lattice makes it a weakly n-doped material. The TiO_2 particle diameter is too small which ensure that the diffusion length is greater than that of the nanocrystalline TiO_2 layer [7]. The electron travels through the outer circuit performing work, reaches the back FTO Electrode (Figure 1.4).

The maximum output voltage equals to the difference between the Fermi level of the semiconductor and the redox potential of the mediator [Fig 1.3]. Thus the device is can produce electricity from light without undergoing any permanent physical and chemical change.

Chapter 2

Study of Dye Sensitized Solar Cell

2.1 Theoretical Modeling of DSSC:

The current-voltage characteristics of DSSC solar cells can be determined by using one diode equivalent circuit (Fig 2.1). It represents very useful model for characterizing electrical parameters of DSSC solar cell [8, 10].

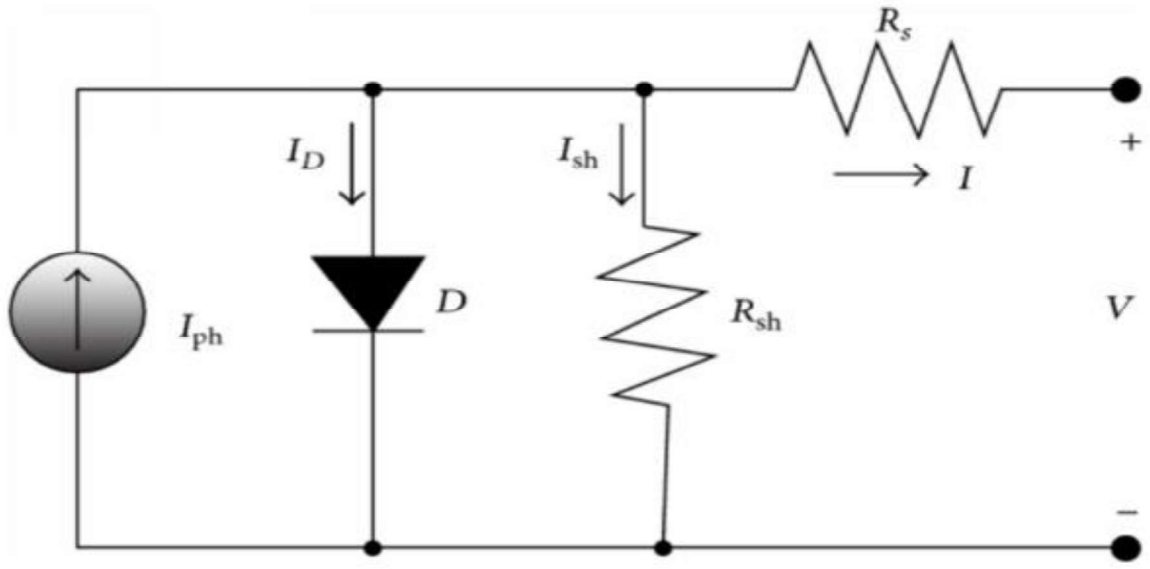

Fig 2.1: One-diode equivalent circuit model of DSSC

From the figure, I-V characteristics can be representing by given equation [9]:

$$I = I_{ph} - I_d - I_p = I_{ph} - I_s\left[\exp\left(\frac{\beta}{n}(V + IR_s)\right) - 1\right] - G_{sh}(V + IR_s) \qquad (1)$$

Where physical parameters are given by:

*R*s = Series resistance,

n = ideality factor,

Rsh = Shunt resistance,

Iph = Photo current,

Is = Saturation current,

β = Inverse thermal voltage (β=q/kT, k=Boltzmann constant, 1.38×10^{-23},T=Temperature, 300K)

Ip =Shunt current,

Gsh = Shunt conductance.

Shunt resistance *Rsh = (1/Gsh) >> Rs*.

Gsh is determined from reverse bias characteristics by a simple linear fit [9].

Shunt current can be calculated from *Gsh, Ip = GshV*.

Determination of n and Rs:

From the linear fit and for *V+RsI>>kT*, the *I-V* relation becomes:

$$I = I_{ph} - I_s\left[\exp\left(\frac{\beta}{n}(V + IR_s)\right)\right] \quad (2)$$

The logarithmic form of eq. 2 can measured directly from *I-V* data.

$$\ln(I_{ph} - I) = \ln I_s + \frac{\beta}{n}(V + IR_s) \quad (3)$$

Determination of *Iph*:

For most practical solar cells, it is usually considered that *Is*<<*Iph*, the short circuit current can be given by the approximation *Isc*~*Iph*.

Determination of *Is*:

The saturation current *Is* is determined from I-V data by plotting *ln*(*Iph*-*Icr*) vs *Vcr* equation:

$$\ln\left(I_{ph} - I_{cr}\right) = \ln(I_s) + \frac{\beta}{n} V_{cr}$$

2.2 Parametric Analysis:

The electrical parameters for DSSC solar cell based on TiO_2 nanostructures and ZnO nanotubes are given below [9]:

Parameters	TiO2 nanostructures	ZnO nanotube
$Gsh(\Omega^{-1})$	0.001269	0.000588
Rs(Ω)	0.025923	0.383441
n	1.629251	3.560949
Is(μA)	0.33556	0.16553
Iph(mA/cm^2)	15.99	3.25

Table 2.1: Extracted parameters for DSSC based on TiO_2 nanostructures and ZnO nanotube.

2.3 Simulation and Discussion:

The extracted parameters are simulated in MATLAB by solving eq1 [10].

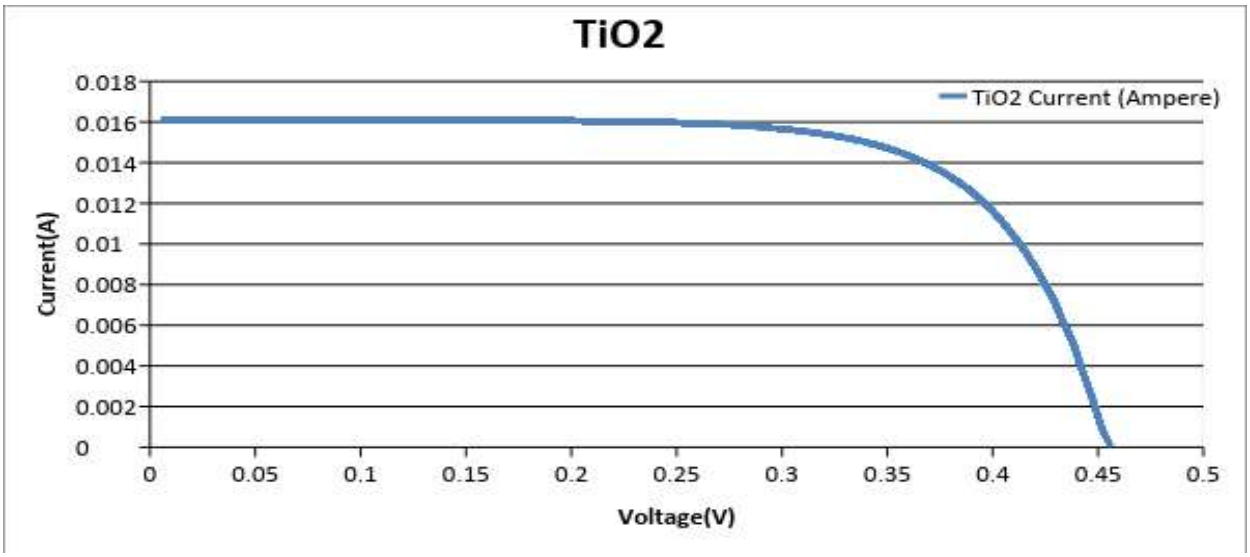

Fig 2.2: I-V curve of TiO2

Fig 2.2 shows the simulated *I-V* characteristic of TiO_2 nanostructure based dye-sensitized solar cell. It is simulated by solving eq.1 and Table 2.2 shows parameters for TiO_2 nanostructure. It shows that for 0.46V open circuit voltage the current *I* is 0.016A.

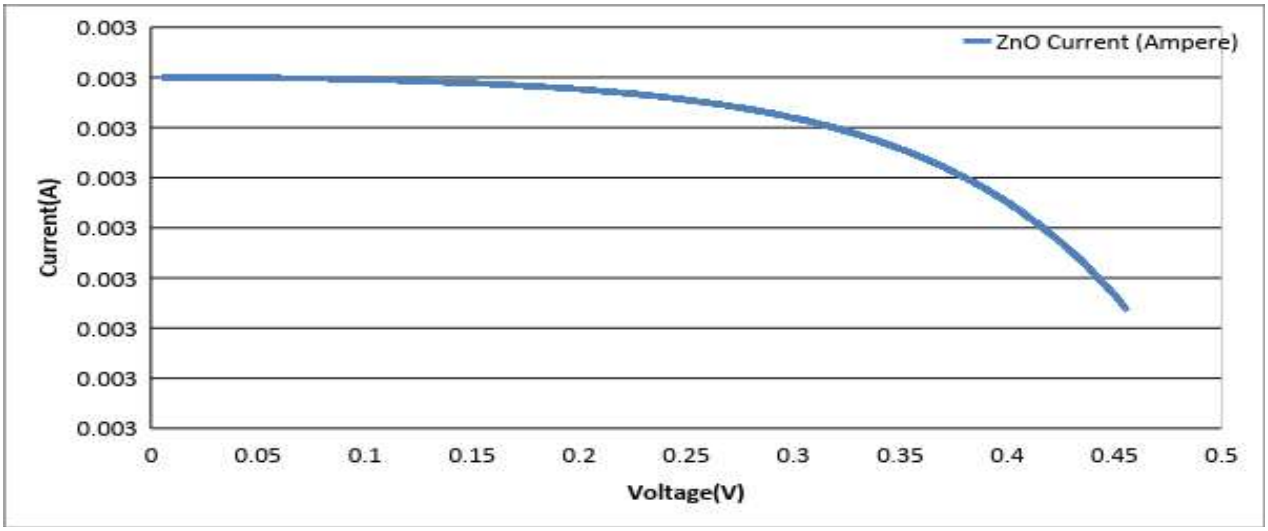

Fig 2.3: *I-V* curve of ZnO

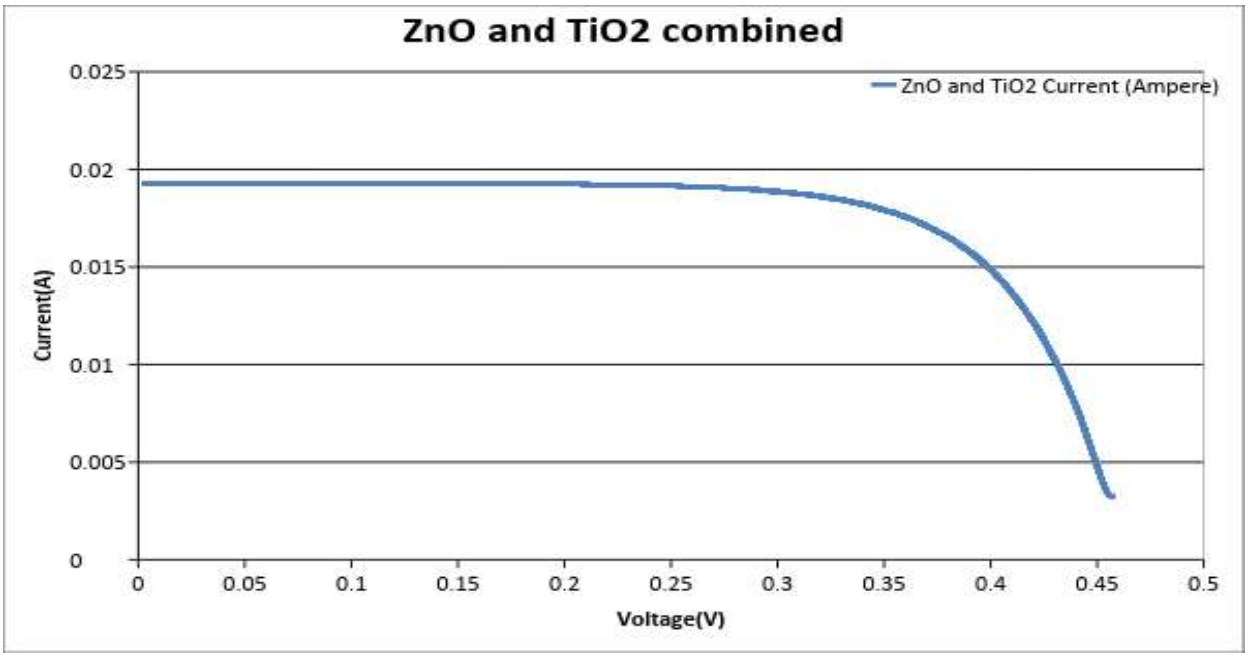

Fig 2.4: *I-V* characteristics of TiO_2 & ZnO combined layer

From Fig 2.4, it is numerically calculate that for TiO_2 and ZnO combined layer the *I-V* characteristics changes significantly. It is observed that current increases approximate 0.02 amps, which is significant. From above figure, it is predicted that for combined layer current and voltage will increase.

2.4 Flowchart Demonstration of I-V Characteristics:

An MATLAB programming based code was developed to determine Current vs. Voltage relationship for analysis. The following flowchart shows the demonstration of coding in MATLAB for I-V characteristics as a sample of ZnO.

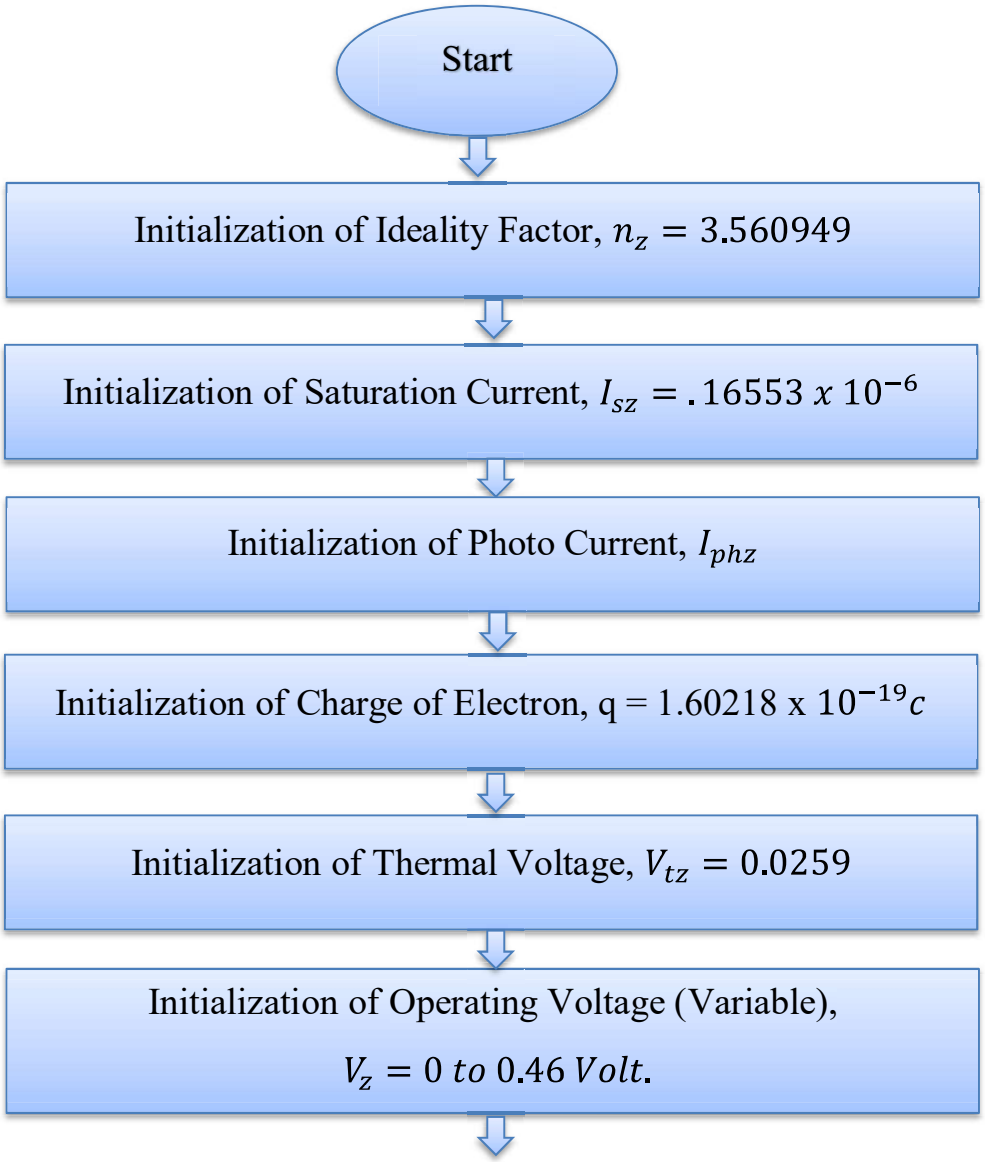

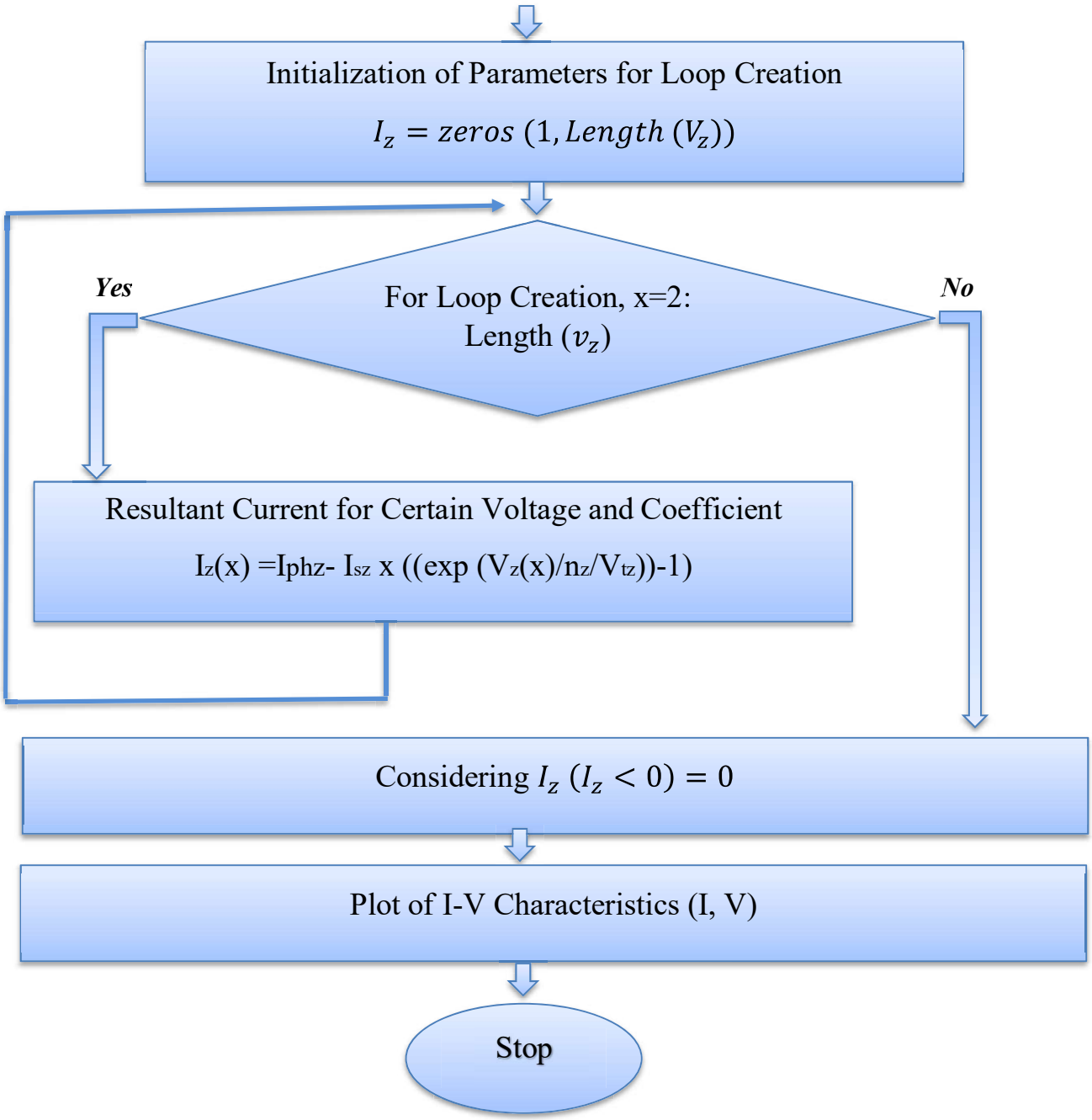
Initialization of Parameters for Loop Creation
$I_z = zeros\ (1, Length\ (V_z))$
For Loop Creation, x=2: Length (v_z)
Yes
No
Resultant Current for Certain Voltage and Coefficient
Iz(x) =Iphz- Isz x ((exp (Vz(x)/nz/Vtz))-1)
Considering $I_z\ (I_z < 0) = 0$
Plot of I-V Characteristics (I, V)
Stop

Chapter 3

Study of Thickness Effect on Dye Sensitized Solar Cell

3.1 Thickness Effect of DSSC:

In this section, we will discuss about the dependence of film thickness on dye-sensitized solar cell. Recently some research article [11, 12] used a mathematical model based on electron diffusion to observe effect of electrode thickness in DSSC. The diffusion model uses to study how the open-circuit voltage varied with different thickness.

3.2 Modeling:

In Sodergren et al [13] research paper he used two equations in his model to observe electron transport, recombination, and generation in nanostructure film [13, 15]:

$$D\frac{\partial^2 n(x)}{\partial x^2} - \frac{n(x)-n_0}{\tau} + \Phi_0 \alpha \exp(-\alpha x) = \frac{\partial n}{\partial t} \quad (1)$$

Here *n(x)* is excess electron concentration at position *x* within the film, *n0* is electron concentration in dark under equilibrium condition (n0 $=10^{16} cm^{-3}$) [15, 17], τ is lifetime of electron conduction band free electrons, ϕ is light intensity, $\boldsymbol{\alpha}$ is light absorption coefficient of porous film, D is electron diffusion length. Under steady state eq.1 becomes [14, 15]:

$$D\frac{\partial^2 n(x)}{\partial x^2} - \frac{n(x)-n_0}{\tau} + \Phi_0 \alpha \exp(-\alpha x) = 0 \quad (2)$$

Electrons are easily extracted as photocurrent and no electrons are drawn directly as counter electrode. Hence, the boundary conditions are:

$$n(0) = n_0 \quad (3)$$

And

$$\left.\frac{dn}{dx}\right|_{x=d} = 0 \quad (4)$$

Here *d* is the thin film of electrode thickness.

Excess electron concentration of the photovoltage, *Vph* given by:

$$\left|V_{ph}\right| = \frac{kT}{q} m \ln \frac{n_{contact}}{n_0} \quad (5)$$

Where k is Boltzmann constant, *m* is ideality factor, *q* is electron charge, and T is temperature.

Now, Short-circuit current density *Jsc* can be calculating by given expression [14, 15]:

$$J_{sc} = \frac{q\Phi L\alpha}{1-L^2\alpha^2}\left[-L\alpha + \tanh\left(\frac{d}{L}\right) + \frac{L\alpha \exp(-d\alpha)}{\cosh(\frac{d}{L})}\right] \quad (6)$$

Where *L* is diffusion length, which can be measured by the following equation,

$$L = \sqrt{D\tau} \quad (7)$$

When DSSC operates under a potential difference *V* between Fermi level and electrolyte redox potential, the density of electrons increases at *x*=0 to *n* which gives the new boundary condition:

$$n(0) = n \quad (8)$$

The second boundary conditions at x=*d* remain unchanged. Now solving eq.2 and eq.5 we get the new boundary condition which yields current and voltage relation:

$$V = \frac{kTm}{q} ln\left[\frac{L(J_{sc}-J)}{qDn_0 \tanh(\frac{d}{L})} + 1\right] \quad (9)$$

The equation can be solved in given form:

$$J = J_{sc} - \frac{qDn_0}{L}\tanh(\frac{d}{L})(\exp\left(\frac{qV}{kTm}\right) - 1) \quad (10)$$

3.3 Calculation of Internal Parameter of DSSC:

The effects of thickness on *J-V* characteristics can be determined from five internal parameters of DSSC. This can be obtained from the practical values of the material properties. Some research article [9] calculated different values for electron diffusion coefficient of porous thin film. D, was equal to $1.0\times10^{-2}cm^2s^{-1}$[15,16]. Gomez and Salvador [11, 12, 15] studied D is equal $2.0\times10^{-5}cm^2s^{-1}$. In our modeling study we will use mid-range value of D, which is about $5.0\times10^{-4}cm^2s^{-1}$[15].Another important parameters for light intensity, $\phi = 1.0\times10^{17}cm^{-2}s^{-1}$ which represents value of 1 sun condition (100 mW/cm^2)[11,12,15].

The referenced values of different parameters for DSSC are given below [11, 12, 14, and 15]:

Parameters	Reference value TiO_2	Reference value ZnO
Light intensity, ϕ ($cm^{-2}s^{-1}$)	1.0×10^{17}	1.0×10^{17}
Diffusion coefficient, D (cm^2s^{-1})	5.0×10^{-4}	5.0×10^{-4}
Light absorption coefficient, $\boldsymbol{\alpha}$ (cm^{-1})	5000	4000
Ideality factor, *m*	4.5	3.5
Electron lifetime, t (ms)	10	40
Electron diffusion length, L ($cm^{-1}s^{-1}$)	2.0747×10^{-3}	1.8441×10^{-3}

3.4 Results and Discussion:

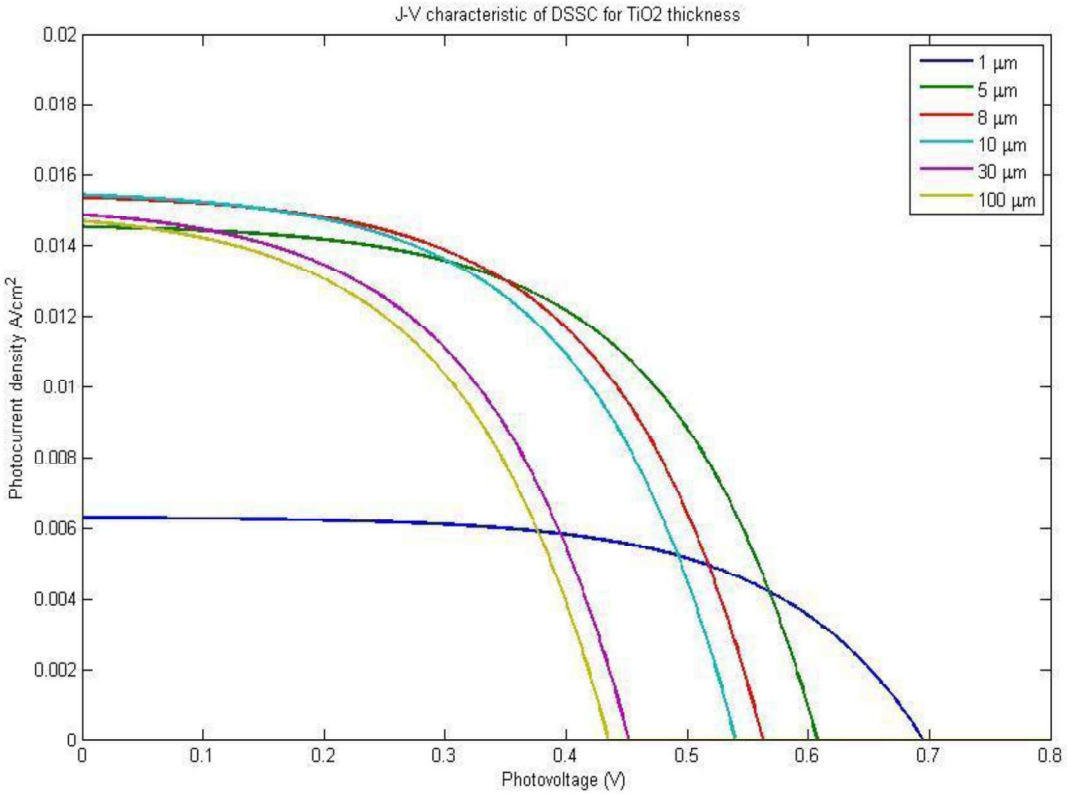

Fig 3.1: *J-V* characteristics for different electrode thickness of TiO_2

J-V characteristics of TiO_2 varying electrode thickness are shown in Fig 3.1. From the plot, it shows that as thickness *d* increases, the current density *Jsc* increases simultaneously, *Jsc* reaches peak point at 10 µm afterwards its decreases gradually. This variation of *Jsc* can be described by electron photogeneration [15], which explains that as thickness increases, it directly increases the internal surface area, resulting a higher dye loading. Hence, it is calculated that thicker electrode absorb more photons, resulting higher *Jsc*. However, *Jsc* cannot increase any further as the number of photons for electron photogeneration reaches the limit. Instead, the increase of electrode thickness beyond light penetration depth causes higher electron loss and gradual reduction in *Jsc*.

The *J-V* plot of TiO_2 also shows that by increasing electrode thickness *d* open circuit voltage *Voc* decreases. It can be explained by electron dilution effect [11, 12]. It describes that when light transmitted through electrode, the light intensity decreases simultaneously. As *d* increases, the electron density becomes lower, which explains *Voc* decreases. The higher resistance works as catalyst to reduction in photovoltage.

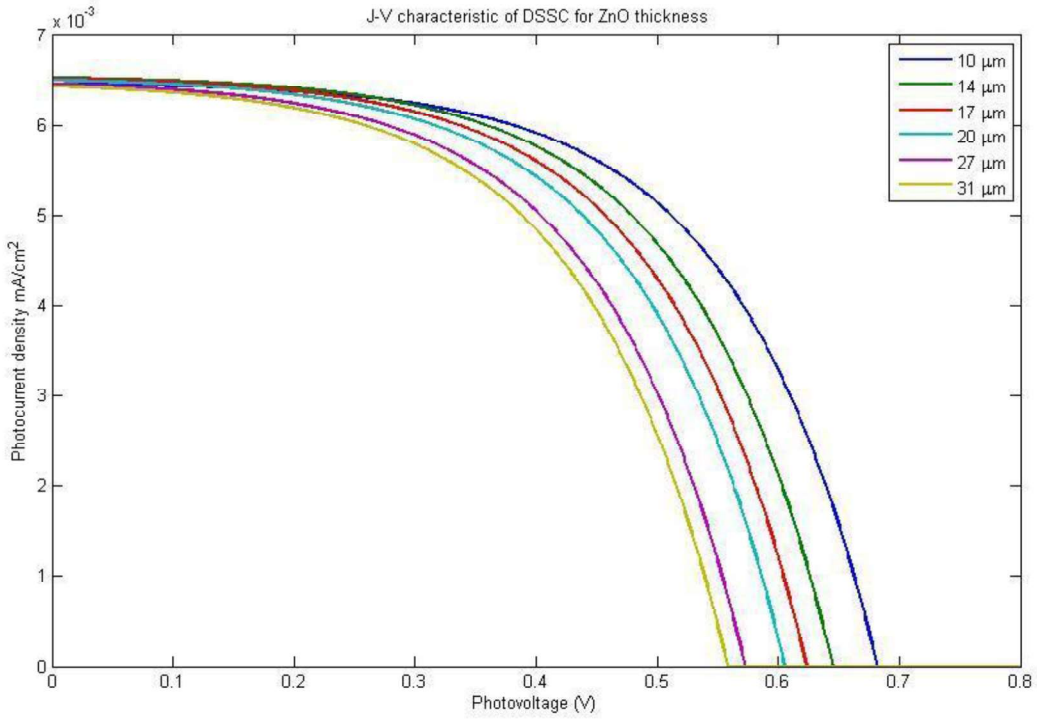

Fig 3.2: *J-V* characteristics for different electrode thickness of ZnO

Fig 3.2 shows the *J-V* characteristics for different electrode thickness of ZnO. It shows the current value reaches peak point at 20µm, which is 0.00656 A/cm^2 and open circuit voltage *Voc* 0.61V.

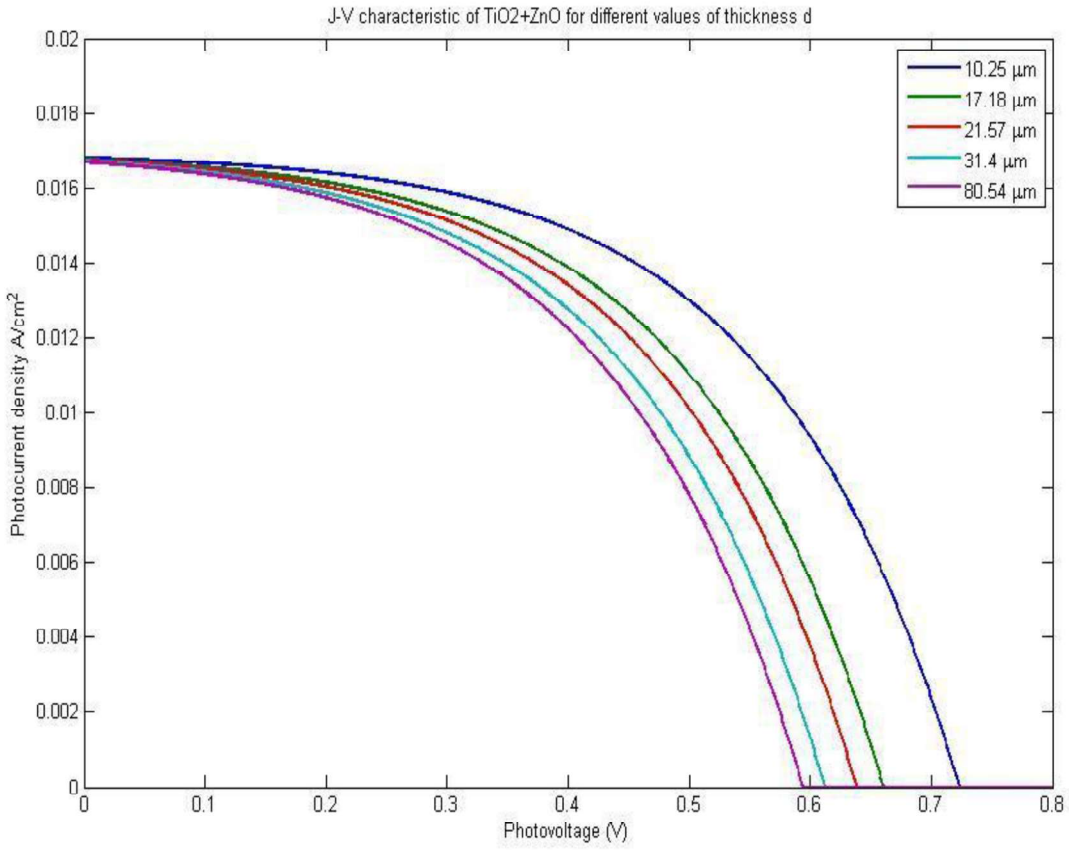

Fig 3.3: *J-V* characteristics for different electrode thickness of TiO_2 & ZnO combined layer

The *J-V* characteristics of ZnO & TiO_2 combined layer shows that at 10.25µm current density and open circuit voltage is maximum (J=0.0168 A/cm^2, Voc= 0.73 V). However, when electrode thickness increases the voltage decreases gradually. However, there is no significant change in current density, Jsc. It explains the electron photogeneration.

3.5 Flowchart Demonstration of Thickness Effect:

An MATLAB programming based code was developed for demonstration of different thickness effect on J-V characteristics. The following flowchart is just a representation of coding.

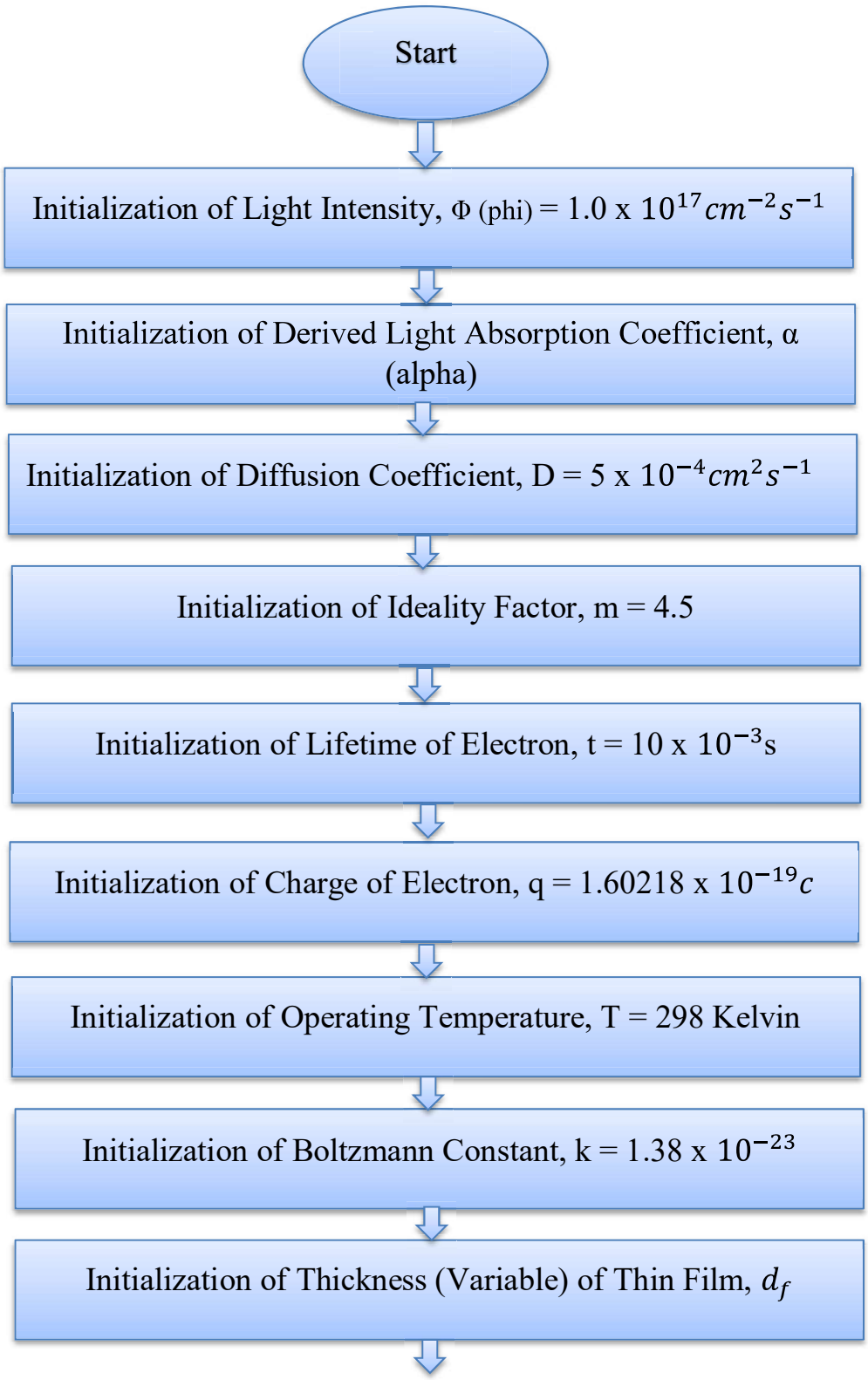

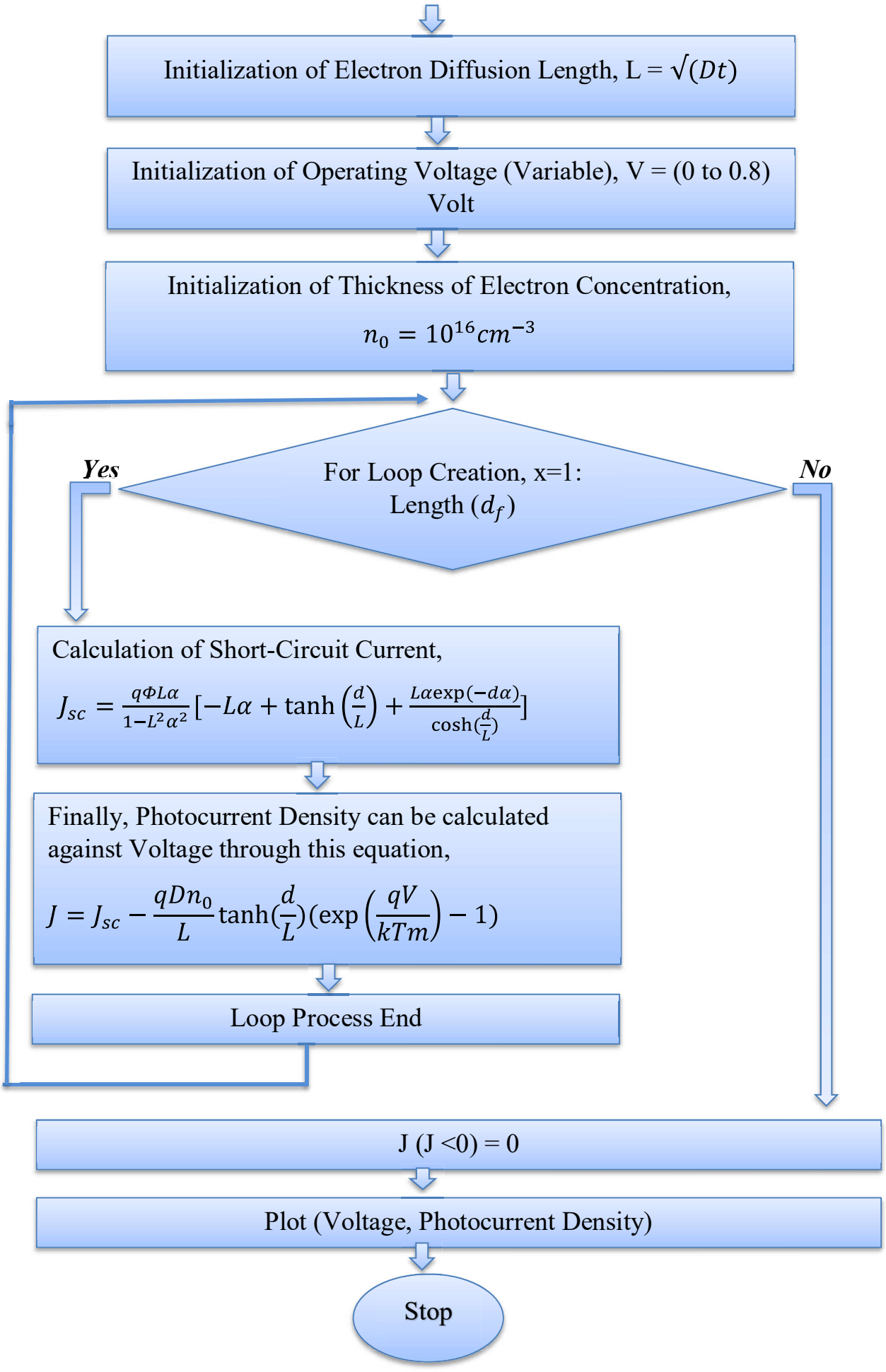
Initialization of Electron Diffusion Length, L = $\sqrt{(Dt)}$
Initialization of Operating Voltage (Variable), V = (0 to 0.8) Volt
Initialization of Thickness of Electron Concentration, $n_0 = 10^{16} cm^{-3}$
For Loop Creation, x=1: Length (d_f)
Yes
No
Calculation of Short-Circuit Current, $J_{sc} = \frac{q\Phi L\alpha}{1-L^2\alpha^2}[-L\alpha + \tanh\left(\frac{d}{L}\right) + \frac{L\alpha\exp(-d\alpha)}{\cosh(\frac{d}{L})}]$
Finally, Photocurrent Density can be calculated against Voltage through this equation, $J = J_{sc} - \frac{qDn_0}{L}\tanh(\frac{d}{L})(\exp\left(\frac{qV}{kTm}\right) - 1)$
Loop Process End
J (J <0) = 0
Plot (Voltage, Photocurrent Density)
Stop

Chapter 4

Optical Transmission Spectrum Analysis

4.1 Introduction to Optical Transmission Spectrum

Semiconductors have significance properties in terms of light absorption for Dye Sensitized Solar Cell (DSSC). Optical thin films are very promising as any preferred reflectance and transmittance properties can be generated through deposition of very thin layer one upon another material or elements [18]. In this case, wide band gap of particular materials has drawn great attractions to researchers and scientists for their own identical properties of light absorption. Dye Sensitized Solar Cell is a third generation solar cell, which is dependent on different type of dyes for its structural configuration. Optimization of thickness, composition, roughness along with various properties is important for prior application [19, 20]. Determination of spectral transmittance and reflectance can be measured through optical property measurements and analysis tool in terms of UV to IR ranges of spectrum [21]. Presently, management of light known as light scattering along with antireflection and trapping of light are much more important factors to develop optimized optoelectronic and photovoltaic devices. [22-24].

4.2 Brief Study of ZnO and TiO_2 Properties

Through having a wide band gap equivalent of 3.37 eV [25], ZnO has promising characteristics for optical photo electrochemical behavior and responses. Being transparent in the visible range of the spectrum is considered as uniqueness for a semiconductor like ZnO [26]. It's really important to investigate the properties of photo electrochemical behavior of a semiconductor like ZnO to know the potentiality and usefulness for DSSC preparation for multi-layer or single layer based solar cell respectively. In this study, we investigated on the absorbance behavior of ZnO Film on glass known as N-BK7 for different wavelengths of UV-vis spectrum to understand its absorbance properties that is inherited in ZnO Film particularly so that we can determine the most effective range of wavelengths to optimize absorbance for the vast performance of DSSC in

layers' construction. We also investigated on the absorbance behavior of TiO_2 Film on FTO glass for different wavelengths of UV-vis spectrum to understand its absorbance properties that is inherited in TiO_2 Film particularly so that we can determine the most effective range of wavelengths to optimize absorbance for the vast performance of DSSC in layers' construction.

4.3 Methodology of ZnO and TiO_2 Absorbance vs. Wavelength Simulation

UV-vis properties of ZnO Film and TiO_2 Film were investigated through analytical equation derivations with several coefficients value extractions and calculations were being performed through MATLAB.

4.4 Parameters Extraction for Simulation

The equations that we used to derive the Absorbance (A.U) for different wavelengths of UV-vis are particularly shown below:

Refractive index of air has been considered as 1.00 for all wavelengths for UV-vis.

Reflectance of ZnO thin film on Glass (N-BK7) and TiO_2 thin film on FTO Glass substrate have been calculated by this formula where Reff [27] is the effective reflectance.

$$R_{eff} = \frac{P^2+Q^2+2PQcosR}{1+P^2Q^2+2PQcosR}$$

Transmittance of ZnO thin film on Glass (N-BK7) and TiO_2 thin film on FTO Glass substrate have been calculated by this formula where T_{eff} [27] is the effective reflectance.

$$T_{eff} = \frac{16{n_0}^2{n_f}^2 n_s}{1+P^2Q^2+2PQcosR}$$

Where, P, Q, R [10] are derived below

$$P = \frac{n_o - n_f}{n_o + n_f}$$

$$Q = \frac{n_f - n_s}{n_f + n_s}$$

$$R = \frac{4\pi}{\lambda} n_f d_f$$

n_0 = Refractive Indices of Surrounding Medium (air) = 1.00 (Constant)

n_f = Refractive Indices of Thin film

n_s = Refractive Indices of Glass

d_f= Thickness of Film Thickness.

Thickness was considered for ZnO Thin Film as 0.2 Micrometer and TiO_2 Thin Film as 7.6 Micrometer respectively as being considered with reference work value.

λ = Wavelength of Electromagnetic Spectrum

Refractive indices of TiO_2 thin films have been calculated through using different wavelengths [28].

Values of Refractive Indices of Glass (N-BK7) [29] have been calculated through Dispersion formula:

$$n^2 - 1 = \frac{1.03961212\lambda^2}{\lambda^2 - 0.00600069867} + \frac{0.231792344\lambda^2}{\lambda^2 - 0.0200179144} + \frac{1.01046945\lambda^2}{\lambda^2 - 103.560653}$$

Refractive indices of ZnO thin film have been calculated through using different wavelengths [29].

Absorption coefficient (α) can be gained through [30]

$$\alpha = \frac{1}{t} \ln \frac{(1-R)^2}{T}$$

Finally, the values of Absorbance (A.U) for specific electromagnetic spectrum known as UV-vis spectrum can be gained through [31]

$$A = \frac{\alpha \times d_f}{2.303}$$

4.5 Simulation Result

The resultant Absorbance (A.U) for ZnO Thin Film on Glass (N-BK7) Substrate at UV-vis Spectrum is illustrated below:

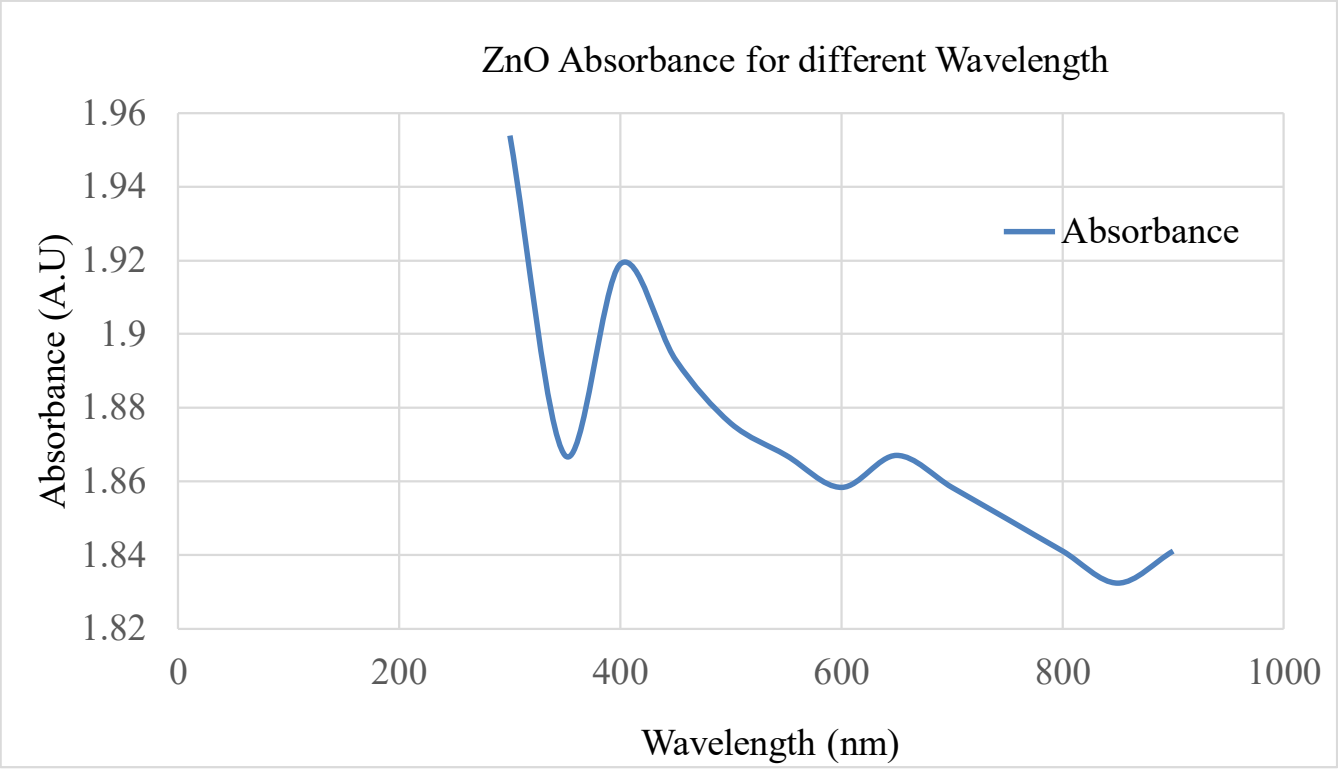

Figure 4.1: ZnO Absorbance for different wavelength of UV-vis spectrum

The resultant Absorbance (A.U) for TiO_2 Thin Film on Glass (FTO) Substrate at UV-vis Spectrum is illustrated below:

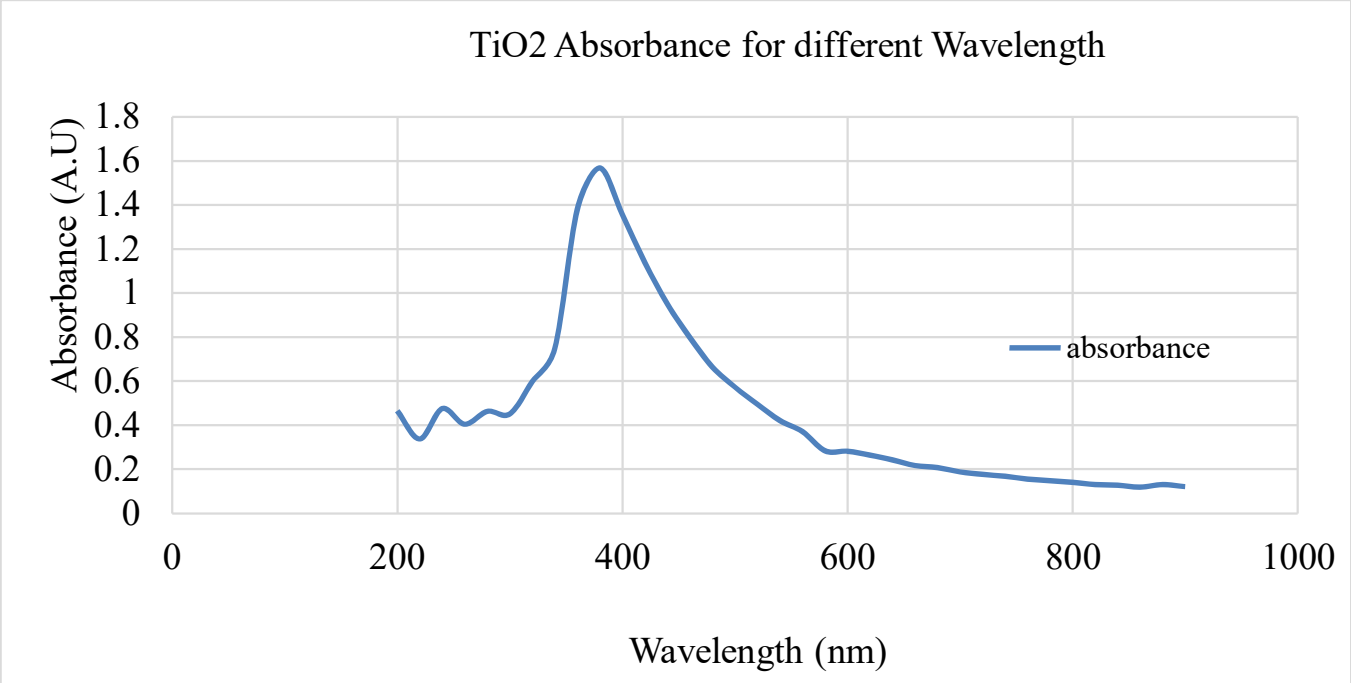

Fig 4.2: TiO2 Absorbance for different wavelength of UV-vis spectrum

4.6 Analysis and Discussion

In this study, we found the maximum absorbance (peak value) of ZnO Thin Film on Glass (N-BK7) substrates for 300 nm of wavelength where absorbance was 1.9539. We found another peak value of absorbance of 1.919 at 400 nm of wavelength. After 400 nm of wavelength, the absorbance is reduced with the increasing values of wavelengths until it reaches to 900 nm (IR Region) where we found the value is slightly increased to 1.8411.

As the simulation is based on the wavelengths of different ranges of UV-vis spectrum, ZnO thin film of .2 micrometers has very sharp and peak absorbance for 300 nm, which is considered as

UV (Ultraviolet region) which implies that ZnO Thin Film of 0.2 micrometer has an exceptional property to absorb the UV spectrum particularly.

On the other hand, in visible spectrum of 400 nm wavelength it is found to be the second highest peak value of absorbance for ZnO thin film and later with increasing wavelength values absorbance just reduced. Significant changes have been identified in UV region and visible region of electromagnetic spectrum due to the transition between the valence band and conduction band particularly.

On the other hand, the simulated result of absorbance for different wavelengths of TiO_2 has been illustrated in figure. From the graph of absorbance for different wavelength, we found the maximum absorbance (peak value) of TiO_2 was 1.5678 for wavelength of 380 nm. We considered another two wavelength points as likely 400 nm and 600 nm for TiO_2 where the absorbance values were identified as 0.4516 and 0.2824 particularly.

From the depth analysis of plotting of absorbance for different wavelength, we have TiO_2 has the properties to absorb the maximum amount of sunlight irradiance at the very beginning of Ultraviolet region. We also noticed from the illustration that absorbance of TiO_2 below 300 nm is not up to mark and after 600 nm; it is not the significant rate of absorbance. The range of absorbance for TiO_2 was optimized from 300 nm to 600 nm from figure.

4.7 Flowchart Demonstration of Optical Transmission Spectrum

An MATLAB programming based code was developed to determine optical transmission spectrum for analysis. The following flowchart shows the demonstration of coding in MATLAB.

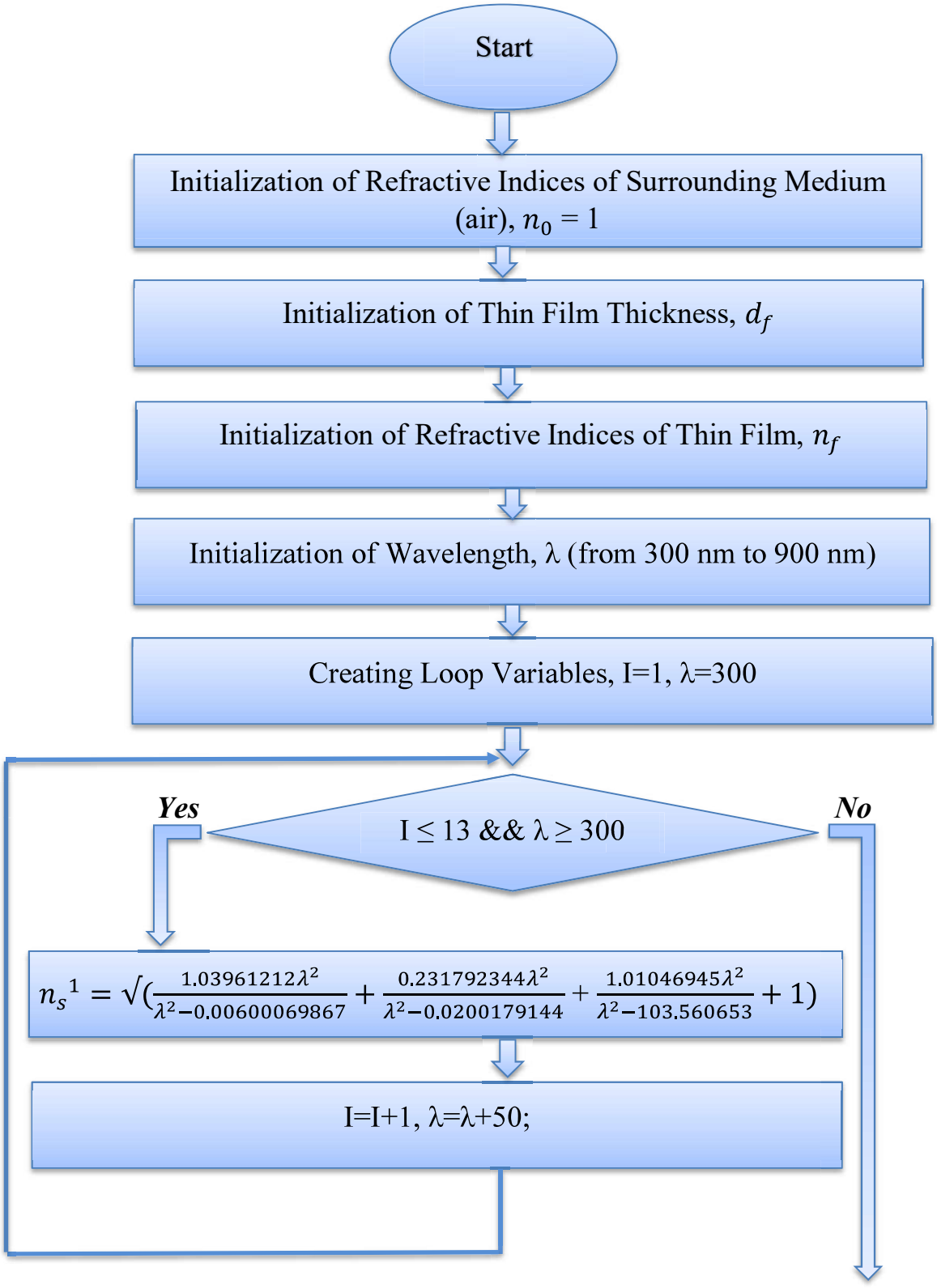

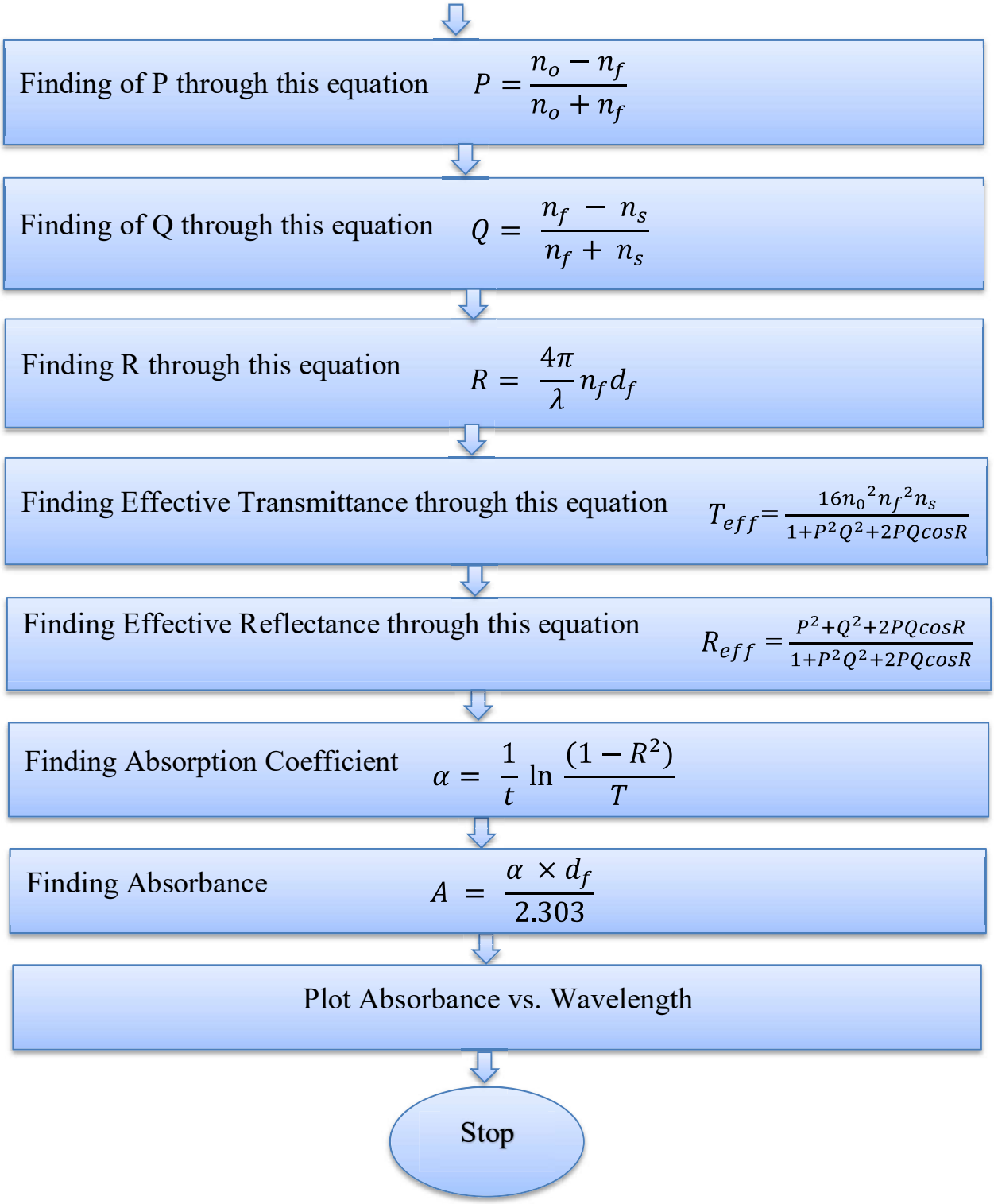
Finding of P through this equation $P = \frac{n_o - n_f}{n_o + n_f}$
Finding of Q through this equation $Q = \frac{n_f - n_s}{n_f + n_s}$
Finding R through this equation $R = \frac{4\pi}{\lambda} n_f d_f$
Finding Effective Transmittance through this equation $T_{eff} = \frac{16 n_0^2 n_f^2 n_s}{1+P^2Q^2+2PQcosR}$
Finding Effective Reflectance through this equation $R_{eff} = \frac{P^2+Q^2+2PQcosR}{1+P^2Q^2+2PQcosR}$
Finding Absorption Coefficient $\alpha = \frac{1}{t} \ln \frac{(1-R^2)}{T}$
Finding Absorbance $A = \frac{\alpha \times d_f}{2.303}$
Plot Absorbance vs. Wavelength
Stop

Chapter 5

JV Characteristics and Performance Analysis

5.1 Introduction to Necessity and Methodology of *J-V* Characteristics

J-V Characteristics is one of the most significant and important analysis of any solar cell particularly for dye sensitized solar cell. As we have already extracted the values of absorption coefficient for maximum absorbance for UV-vis spectrum previously for particular wavelengths respective to TiO_2 and ZnO, our core objective is to investigate the *J-V* characteristics once again to find out if we have any significant changes in *J-V* characteristics based on our extracted parameters values. In our detailed study, we found the parameters values for *J-V* characteristics that are denoted below with proper annotations.

5.2 Extracted Parameters for *J-V* Analysis

Φ (phi) = 1.00×10^{17} ($cm^{-2}s^{-1}$) [32]

Absorption coefficient for TiO_2 (α) = [4498 6800 4279] (cm^{-1}), Thickness 7.6 micrometer

Absorption coefficient for ZnO (α) = [2250 2240 2210] (cm^{-1}), Thickness 0.2 micrometer

Temperature (Kelvin) = 300 K was considered for both materials.

n0 = 1.00×10^{16} (cm^{-3}) was considered for both materials

Thickness of TiO_2, *d* = 7.6 μm

Thickness of ZnO, *d* = 0.2 μm

5.3 Results of Comparative Simulation

The resultant *J-V* characteristic of TiO_2 for particular absorption coefficient of wavelength 300nm, 400nm and 600 nm is illustrated below:

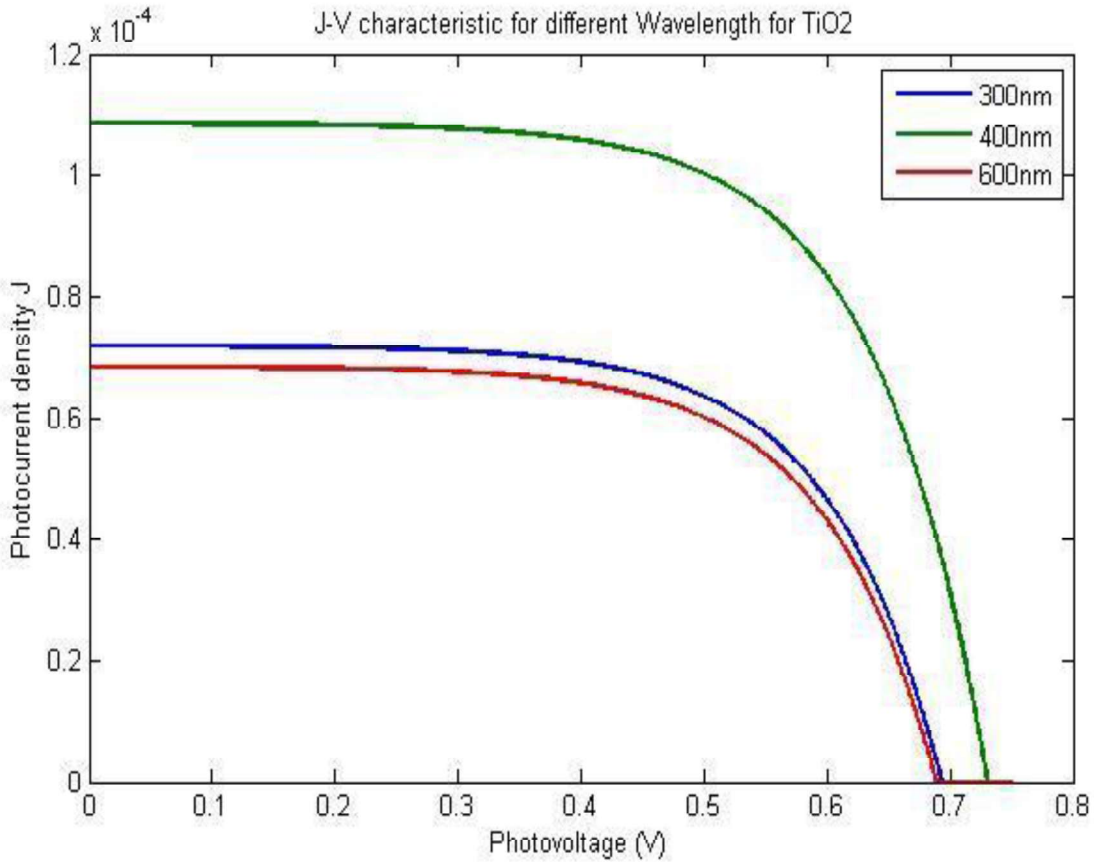

Fig 5.1: *J-V* characteristics for different wavelength of TiO_2

The resultant *J-V* characteristic of ZnO for particular absorption coefficient of wavelength 300nm, 400nm and 600 nm is illustrated below:

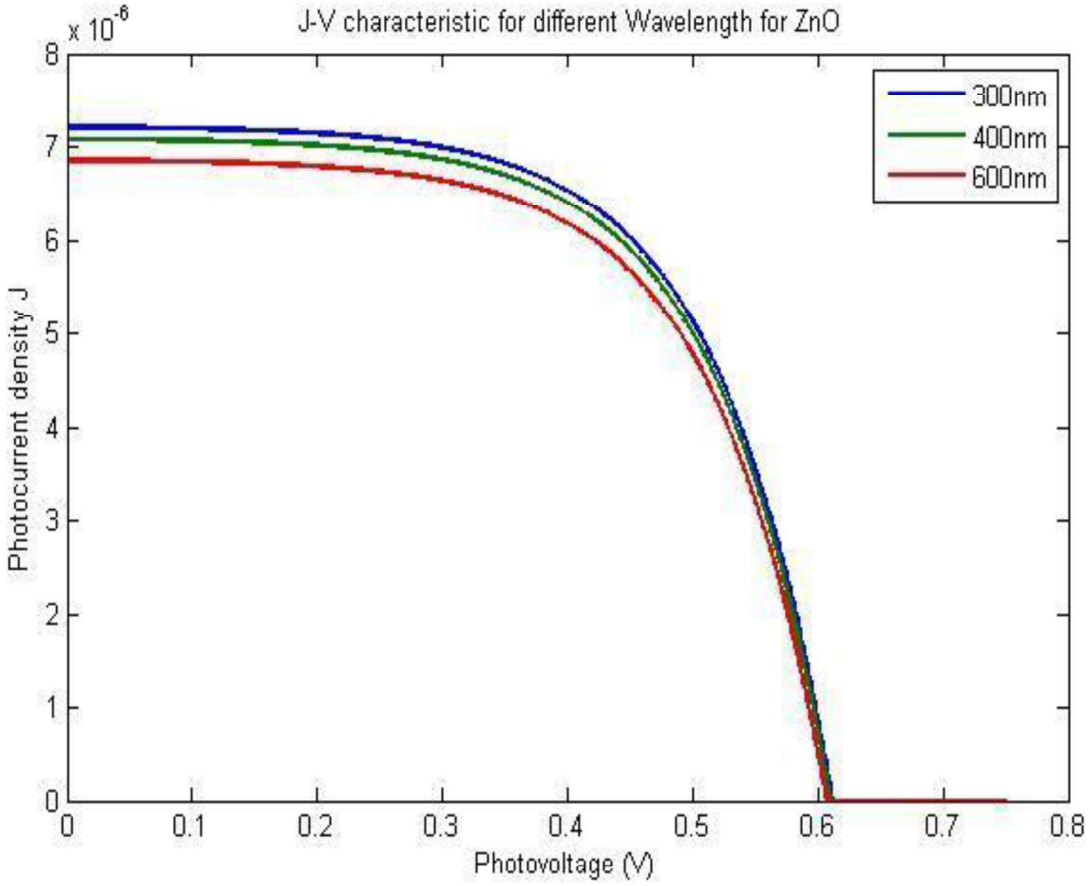

Fig 5.2: *J-V* characteristics for different wavelength of ZnO

The resultant *J-V* characteristics of ZnO and TiO_2 composited materials together for particular absorption coefficient of wavelength 300nm, 400nm and 600 nm is illustrated below:

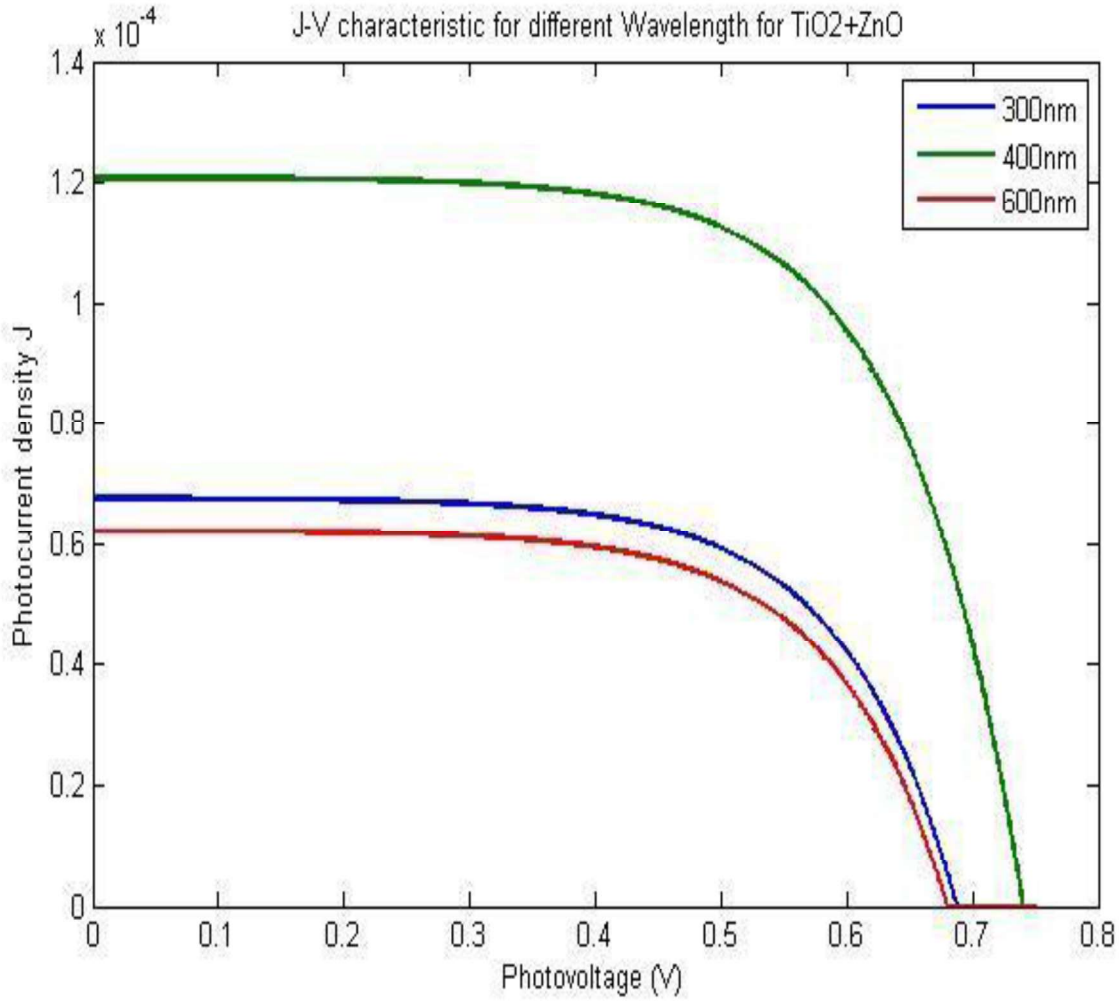

Fig 5.3: *J-V* characteristics for different wavelength of TiO_2 & ZnO combined

As the *J-V* characteristics is dependent on the material thickness, so we have also simulated *J-V* characteristics for TiO_2 and ZnO of 10 micrometer having thickness separately. We also investigated the composited TiO_2 and ZnO along with thickness of 10 micrometers in total to identify the performance and comparative analysis was done.

The resultant *J-V* characteristic of TiO_2 for particular absorption coefficient of wavelength 300nm, 400nm and 600 nm is illustrated below:

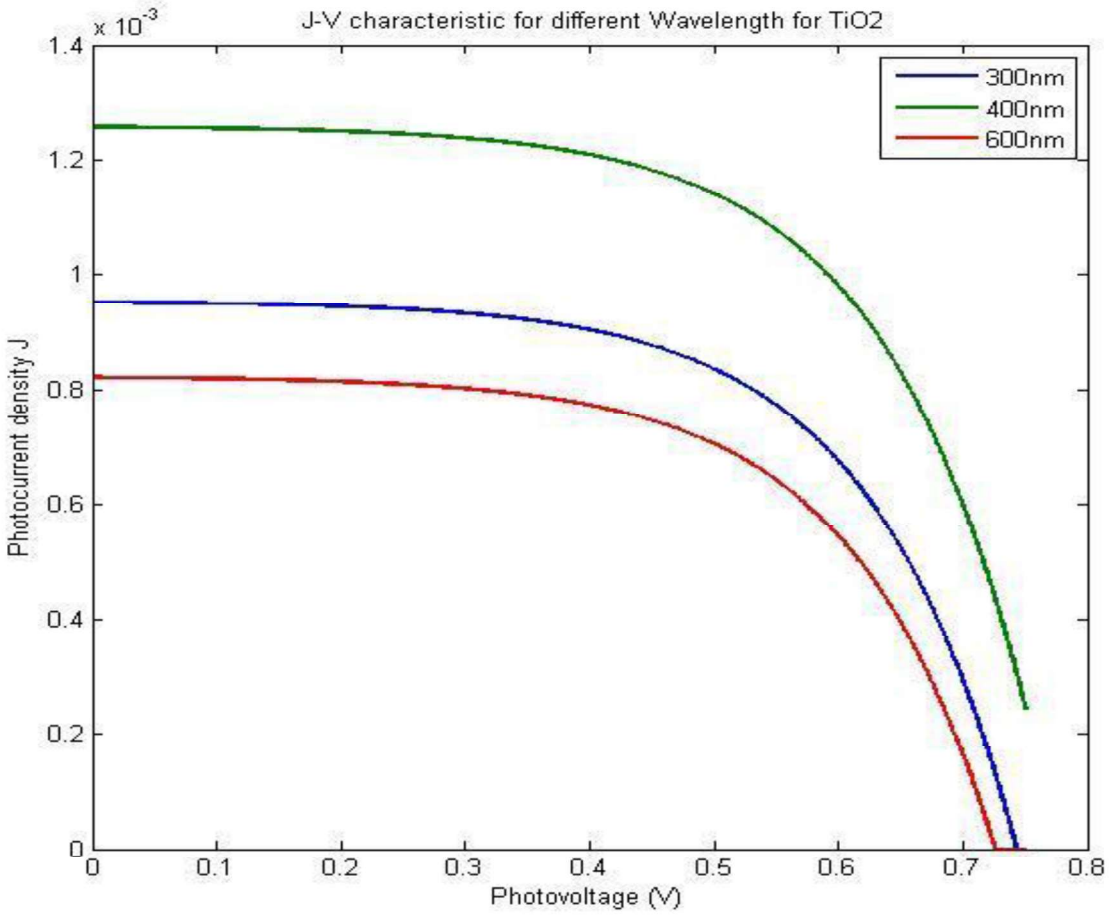

Fig 5.4: *J-V* characteristics for different wavelength of TiO2

The resultant *J-V* characteristics of ZnO for particular absorption coefficient of wavelength 300nm, 400nm and 600 nm are illustrated below:

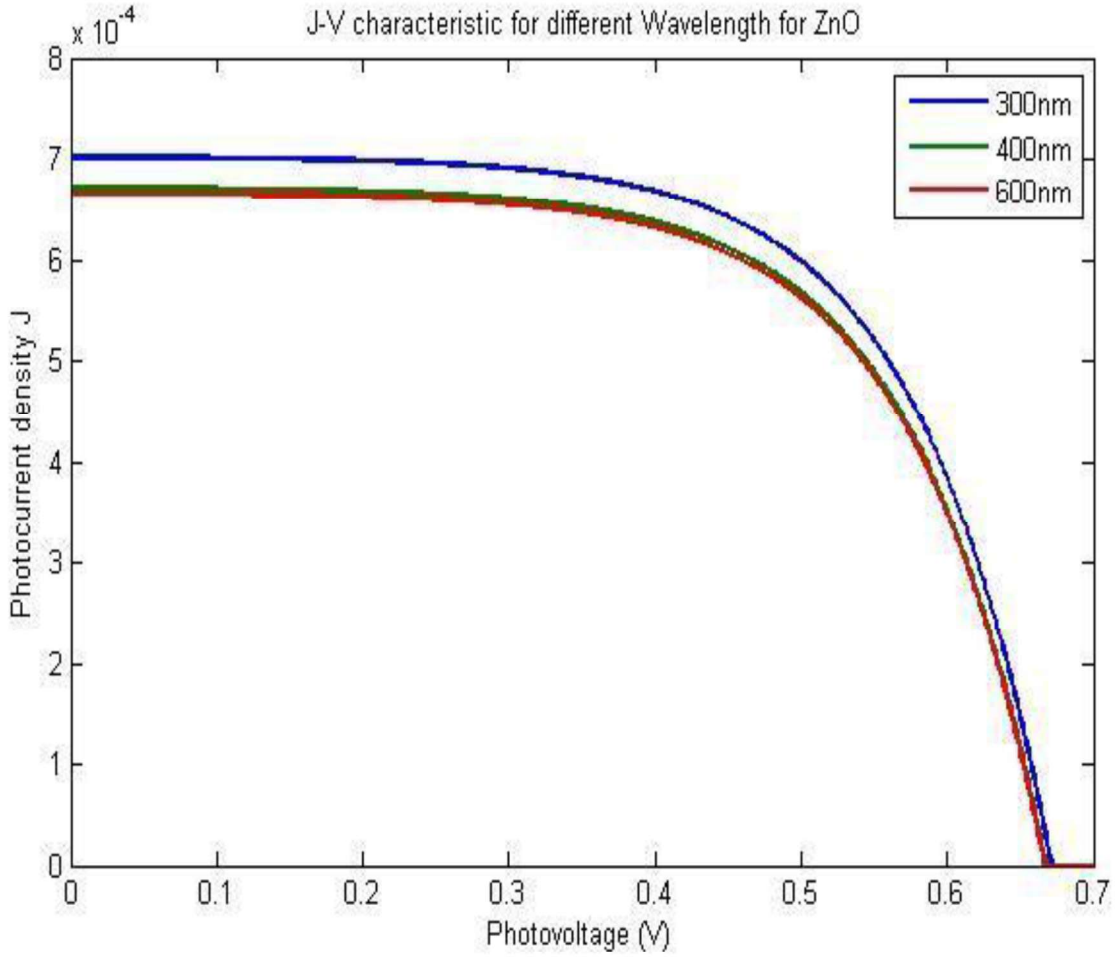

Fig 5.5: *J-V* characteristics for different wavelength of ZnO

The resultant *J-V* characteristics of ZnO and TiO_2 composite materials together for particular absorption coefficient of wavelength 300nm, 400nm and 600 nm is illustrated below:

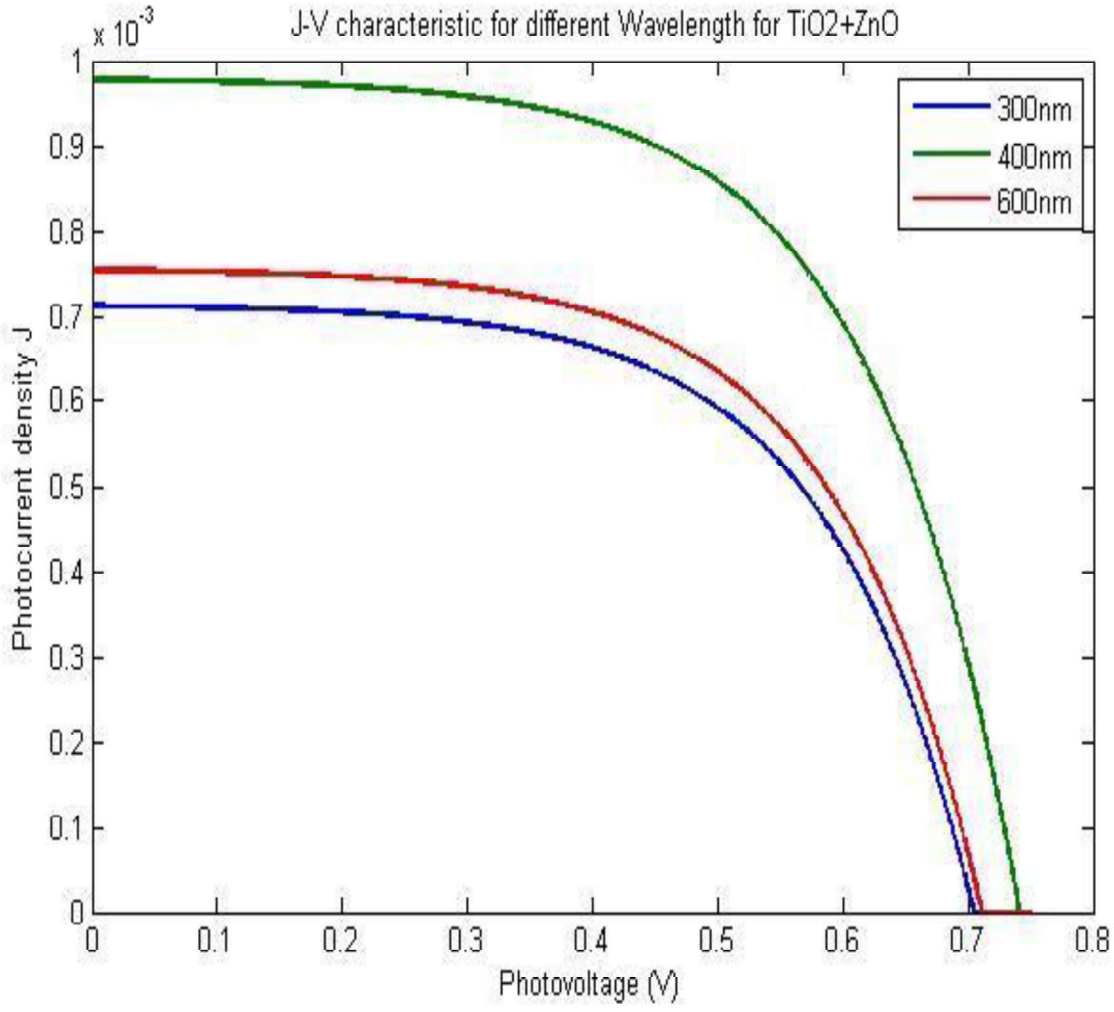

Fig 5.6: *J-V* characteristics for different wavelength of TiO_2 & ZnO combined

5.4 Analysis and Discussion:

Wavelength, λ (nm)	TiO_2 (J, V) Thickness 7.6 μm (micrometer)	ZnO (J, V) Thickness 0.2 μm (micrometer)	TiO_2 and ZnO (J, V) Thickness 7.8 μm (micrometer)
300	J = 0.73 x 10^{-4} $A\ cm^{-2}$ V = 0.68 Volt	J = 7.238 x 10^{-4} $A\ cm^{-2}$ V = 0.61 Volt	J = 0.687 x 10^{-4} $A\ cm^{-2}$ V = 0.69 Volt
400	J = 1.09 x 10^{-4} $A\ cm^{-2}$ V = 0.73 Volt	J = 7.15 x 10^{-6} $A\ cm^{-2}$ V = 0.608 Volt	J = 1.215 x 10^{-4} $A\ cm^{-2}$ V = 0.74 Volt
600	J = 0.69 x 10^{-4} $A\ cm^{-2}$ V = 0.67 Volt	J = 6.85 x 10^{-6} $A\ cm^{-2}$ V = 0.607 Volt	J = 0.63 x 10^{-4} $A\ cm^{-2}$ V = 0.68 Volt

Wavelength, λ (nm)	TiO_2 (J, V) Thickness 10 μm (micrometer)	ZnO (J, V) Thickness 10 μm (micrometer)	TiO_2 and ZnO (J, V) Thickness 10 μm (micrometer)
300	J = 0.95 x 10^{-3} $A\ cm^{-2}$ V = 0.74 Volt	J = 7 x 10^{-4} $A\ cm^{-2}$ V = 0.67 Volt	J = 0.72 x 10^{-3} $A\ cm^{-2}$ V = 0.71 Volt
400	J = 1.282 x 10^{-3} $A\ cm^{-2}$ V = 0.77 Volt	J = 6.68 x 10^{-4} $A\ cm^{-2}$ V = 0.664 Volt	J = 0.987 x 10^{-3} $A\ cm^{-2}$ V = 0.747 Volt
600	J = 0.82 x 10^{-3} $A\ cm^{-2}$ V = 0.73 Volt	J = 6.65 x 10^{-4} $A\ cm^{-2}$ V = 0.6632 Volt	J = 0.752 x 10^{-3} $A\ cm^{-2}$ V = 0.72 Volt

Simulated result for particular wavelengths has been denoted in tabular format above. From the simulated values it's clear enough to understand the significant changes for TiO_2 and ZnO composited dye sensitized solar cell *J-V* characteristics.

The absorbance of ZnO was maximum for 300 nm wavelengths and particularly in simulated study of *J* and *V* analysis we also found the maximum *J* and *V* on that point. The absorbance of TiO_2 was maximum for 380-400 nm wavelengths and particularly in simulated study of *J* and *V* analysis we also found the maximum *J* and *V* on that point.

Finally, the resultant simulated *J* and *V* analysis of TiO_2 and ZnO composited together had significant changes due to maximum absorption coefficient and absorbance for 400 nm of wavelength.

Again we simulated the *J-V* characteristics for thickness 10 micrometer separately of TiO_2, ZnO and TiO_2 along with ZnO. From our study we found that changing the thickness of the thin films to 10 micrometer has significant performance improvement respective to photocurrent density along with voltage. On other hand, for thickness of 10 micrometer of composited TiO_2 and ZnO maximum photocurrent and voltage was found for the wavelength of 400 nm and least was for 300 nanometer.

From our analytical comparative simulation study, it is clearly visible that combination of TiO_2 and ZnO composite has optimized absorbance property from 380-400 nm range of wavelength where *J* and *V* both are significant. On other hand, combined composite materials likely TiO_2 and ZnO together have shown the properties to absorb the visible spectrum and UV spectrum of particular ranges as their own optical transmission properties are different from each other.

High band gap of both TiO_2 and ZnO have advantages to absorb the different regions of Ultraviolet electromagnetic wavelength light where ZnO has shown more absorbance in terms of light absorption in context. On the other hand, ZnO has comparative advantage of Infrared electromagnetic light absorption. Layer diffusion one upon another has tremendous importance in the context of *J-V* performance improvement though other coefficients and factors like thickness, diffusion length of electron have strong interfere in the field of *J-V* performance evaluation respectively.

5.5 Flowchart Demonstration of Absorbance Effect in JV Characteristics:

An MATLAB programming based code was developed to determine the effect of Absorbance in JV characteristics and for that JV characteristics was analyzed based on the values derived from Optical Transmission Spectrum, which had been discussed previously.

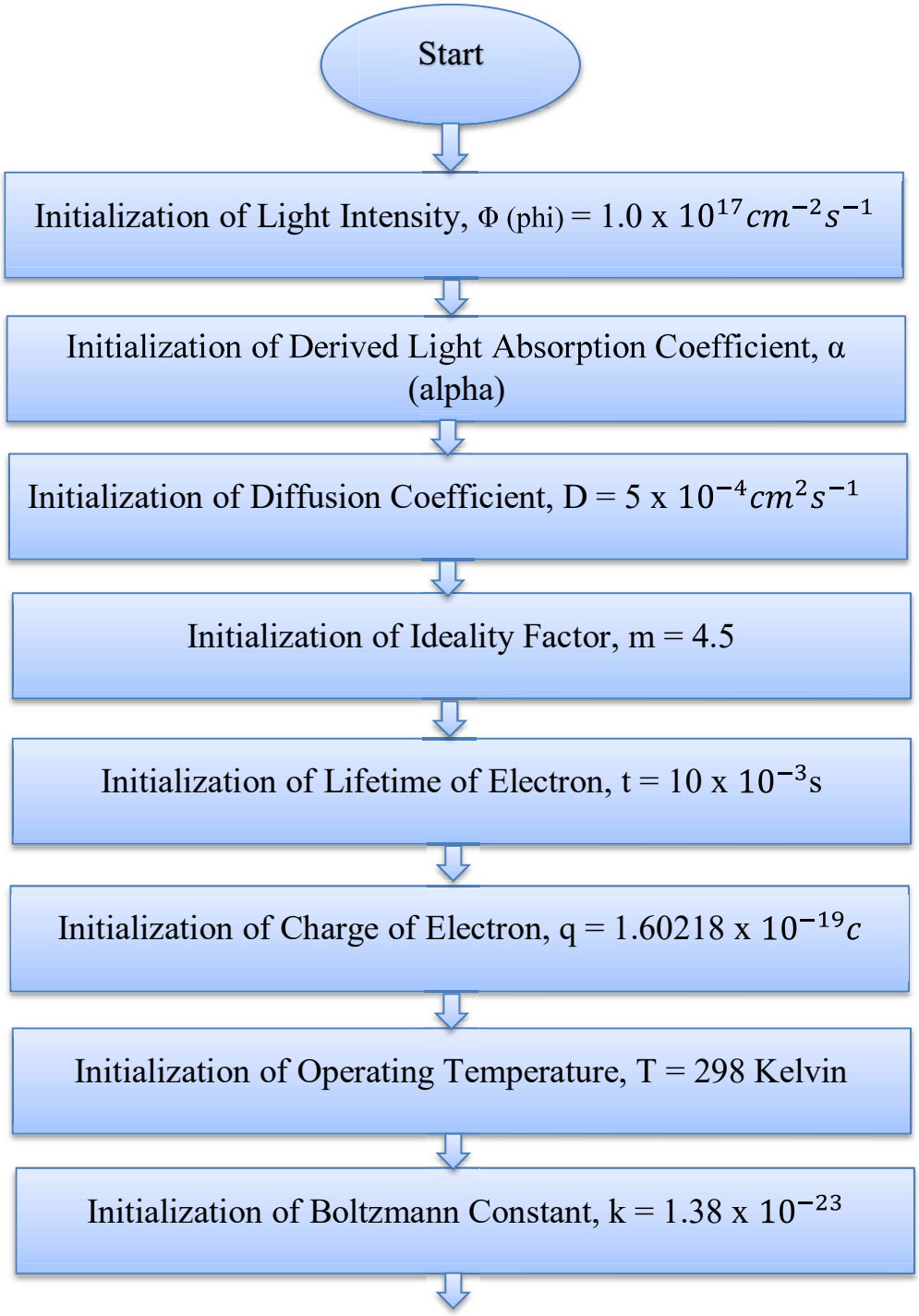

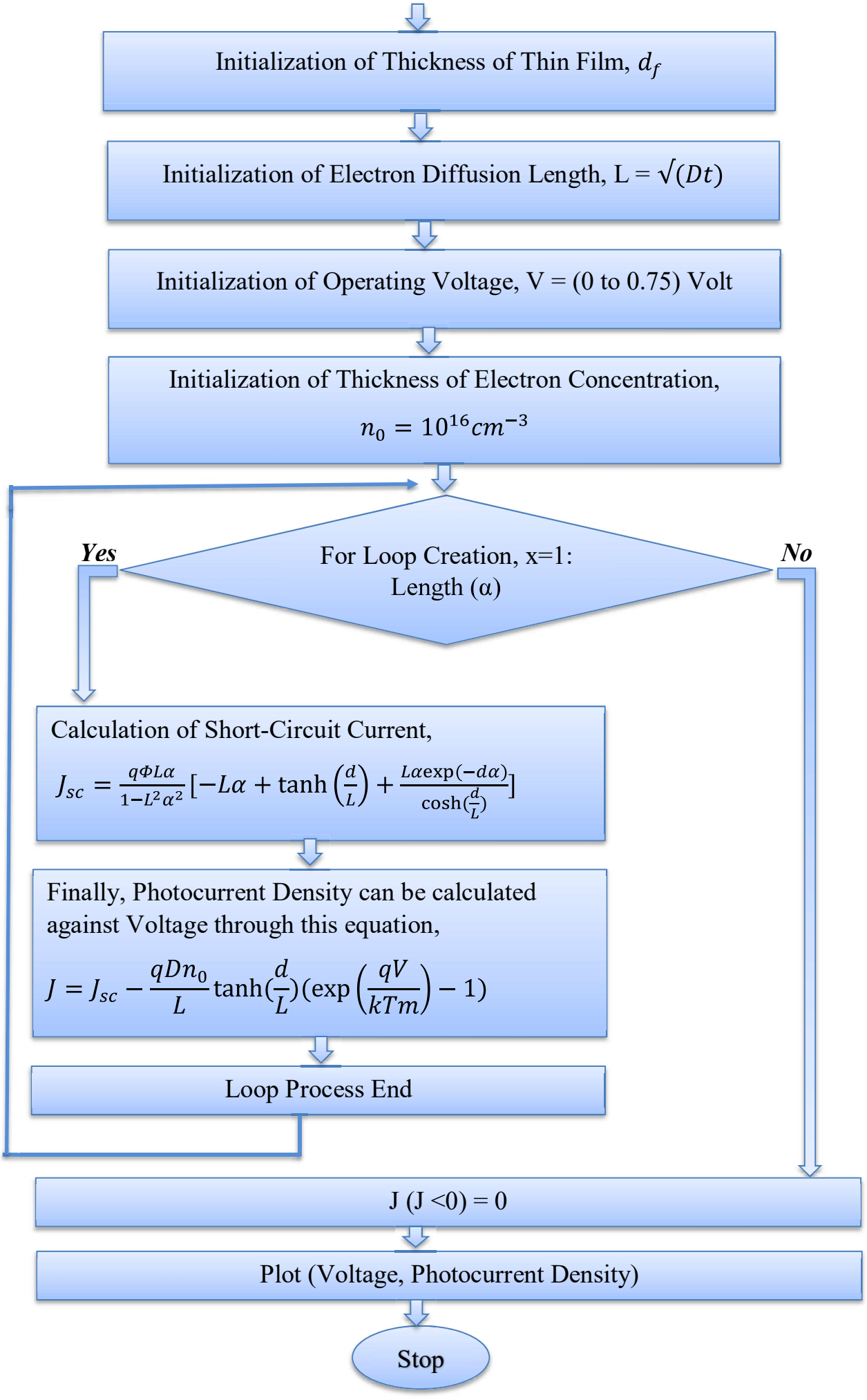
Initialization of Thickness of Thin Film, d_f
Initialization of Electron Diffusion Length, L = $\sqrt{(Dt)}$
Initialization of Operating Voltage, V = (0 to 0.75) Volt
Initialization of Thickness of Electron Concentration,
$n_0 = 10^{16} cm^{-3}$
For Loop Creation, x=1: Length (α)
Yes
No
Calculation of Short-Circuit Current,
$J_{sc} = \frac{q\Phi L\alpha}{1-L^2\alpha^2}[-L\alpha + \tanh\left(\frac{d}{L}\right) + \frac{L\alpha\exp(-d\alpha)}{\cosh(\frac{d}{L})}]$
Finally, Photocurrent Density can be calculated against Voltage through this equation,
$J = J_{sc} - \frac{qDn_0}{L}\tanh(\frac{d}{L})(\exp\left(\frac{qV}{kTm}\right) - 1)$
Loop Process End
J (J <0) = 0
Plot (Voltage, Photocurrent Density)
Stop

Chapter 6

Conclusion and Further Scope

Dye Sensitized Solar Cell (DSSC) known as Grätzel Cell has gained vast attractions to researchers and scientists for its flexibility, stability and cheap materials that are abundant in nature particularly. A simulation model was developed based on the theoretical derived equations and implemented in MATLAB through coding where the parametric coefficients were determined through proper calculations. At the very beginning of thesis work, *I-V* characteristics were investigated for TiO_2, ZnO and for both using the values from reference sources. Analysis of I-V characteristics were evaluated through comparative study.

Throughout the thesis work our core concern was to evaluate the performance of *J-V* characteristics for different values of thickness on TiO_2, Zno and on both materials combination. Optimized thickness for improving *J-V* performance on TiO2 was found as 10 micrometers. On other hand, the optimized thickness for improving *J-V* performance on ZnO was found to be 27 micrometers and finally 10.25 micrometer thickness were found as an optimized thickness for both combinations. Effect of UV-vis spectrum on ZnO and TiO_2 thin film were investigated where comparative analytical study was done.

Finally, we studied the *J-V* characteristics with the optimized thickness along with resultant absorption coefficient derived from Absorbance vs. Wavelength properties. Through simulation we got to know that higher absorption leads to higher *J-V* characteristics for thin films particularly. Optimized thickness was found to be 10 micrometers for thin film materials and wavelength was basically 300 to 400 nanometers of electromagnetic light wave. Combination of TiO_2 photoanode and ZnO compact layer had significant changes in terms of improving *I-V, J-V* and absorption in respective fields.

Extracting the parametric equations co-efficient was complex and challenging at the same time though experimental work on dye sensitized solar cell got maximum attentions to researchers nowadays. Throughout, the whole simulation temperature was considered constant as 300 kelvins. From our study, we also learned that thickness is very important and role playing factor in improvement of *J-V* characteristics and also for absorption.

Study on dye sensitized solar cell is very much interesting and has huge scope to research in further stage. As we have considered temperature constant previously, another simulation can be done by varying the temperatures and investigating the effect of temperatures on *J-V* characteristics for combination of ZnO compact layer and TiO_2 photoanode. Varying the intensity of irradiation of *J-V* characteristics can also be investigated in further stage. Fabrication of ZnO compact layer and TiO_2 photoanode is mandatory for further investigation with comparative analysis with simulation results. Different photoanode can be used as multi-layer deposition and varying glass substrates can enhance performance of dye sensitized solar cell.

Reference:

1. Graetzel, Michael. (2004). Conversion of Sunlight to Electric Power by Nanocrystalline Dye-Sensitized Solar Cells. Journal of Photochemistry and Photobiology A: Chemistry. 164. 3-14. 10.1016/j.jphotochem.2004.02.023.
2. Ghani, Faisal & Rosengarten, G & Duke, Mike & Carson, James. (2014). The numerical calculation of single-diode solar-cell modelling parameters. Renewable Energy. 72. 105–112. 10.1016/j.renene.2014.06.035.
3. Green, Martin. (2002). Third generation photovoltaics: Solar cells for 2020 and beyond. Physica E: Low-dimensional Systems and Nanostructures. 14. 65-70. 10.1016/S1386-9477(02)00361-2.
4. Chou, Jung-Chuan & Lin, Yu-Jen & Liao, Yi-Hung & Lai, Chih-Hsien & Chu, Chia-Ming & You, Pei-Hong & Nien, Yu-Hsun. (2016). Photovoltaic Performance Analysis of Dye-Sensitized Solar Cell With ZnO Compact Layer and TiO2/Graphene Oxide Composite Photoanode. IEEE Journal of the Electron Devices Society. PP. 1-1. 10.1109/JEDS.2016.2614940.
5. Taguchi, Taketo & Zhang, Xintong & Sutanto, Irwan & Tokuhiro, Ken-ichi & N Rao, Tata & Watanabe, Hiroko & Nakamori, Toshie & Uragami, Masayuki & Fujishima, Akira. (2003). Improving the performance of solid-state dye-sensitized solar cell using MgO-coated TiO2 nanoporous film. Chemical communications (Cambridge, England). 9. 2480-1. 10.1039/B306118C.
6. Ito, Seigo. (2011). Investigation of Dyes for Dye-Sensitized Solar Cells: Ruthenium-Complex Dyes, Metal-Free Dyes, Metal-Complex Porphyrin Dyes and Natural Dyes. 10.5772/19960.
7. Nazeeruddin, Mohammad & Baranoff, Etienne & Grätzel, Michael. (2011). Dye-sensitized solar cells: A brief overview. Solar Energy. 85. 1172–1178. 10.1016/j.solener.2011.01.018.
8. Nehaoua, N & Chergui, Yahia & E. Mekki, D. (2011). A New Model for Extracting the Physical Parameters from I-V Curves of Organic and Inorganic Solar Cells. 10.5772/24854.

9. Chergui, Yahia. (2015). Photovoltaic Characteristics of ZnO Nanotube Dye-Sensitized Solar Cells and TiO 2 Nanostructure.. 10.13140/RG.2.1.1535.8889.
10. Y. Belkassmi, A. Rafiki, K. Gueraoui, L. Elmaimouni, O. Tata and N. Hassanain, "Modeling and simulation of photovoltaic module based on one diode model using Matlab/Simulink," *2017 International Conference on Engineering & MIS (ICEMIS)*, Monastir, 2017, pp. 1-6. doi: 10.1109/ICEMIS.2017.8272965
11. Gómez, Roberto & Salvador, Pedro. (2005). Photovoltage Dependence on Film Thickness and Type of Illumination in Nanoporous Thin Film Electrodes According to a Simple Diffusion Model. Solar Energy Materials and Solar Cells - SOLAR ENERG MATER SOLAR CELLS. 88. 377-388. 10.1016/j.solmat.2004.11.008.
12. Current Density versus Potential Characteristics of Dye-Sensitized Nanostructured Semiconductor Photoelectrodes. 2. Simulations Jae-Joon Lee,†,§, George M. Coia,*,‡ and, and Nathan S. Lewis*,†*The Journal of Physical Chemistry B* **2004** *108* (17), 52825293 DOI: 10.1021/jp035195m
13. Soedergren, S., Hagfeldt, A., Olsson, J., & Lindquist, S. (1994). Theoretical Models for the Action Spectrum and the Current-Voltage Characteristics of Microporous Semiconductor Films in Photoelectrochemical Cells. *The Journal of Physical Chemistry, 98*(21), 5552-5556. doi:10.1021/j100072a023
14. El Tayyan, Ahmed. (2011). Dye sensitized solar cell: Parameters calculation and model integration. Journal of Electron Devices. 11. 616-624.
15. Ni, Meng & Leung, Michael K.H. & Leung, Dennis. (2008). Theoretical modelling of the electrode thickness effect on maximum power point of dye-sensitized solar cell. The Canadian Journal of Chemical Engineering. 86. 35 - 42. 10.1002/cjce.20015.
16. 05/02166 Brownian dynamics simulations of electrons and ions in mesoporous films. (2005). *Fuel and Energy Abstracts, 46*(5), 318. doi:10.1016/s0140-6701(05)82175-7
17. Rothenberger, G., Fitzmaurice, D., & Graetzel, M. (1992). Spectroscopy of conduction band electrons in transparent metal oxide semiconductor films: Optical determination of the flatband potential of colloidal titanium dioxide films. *The Journal of Physical Chemistry, 96*(14), 5983-5986. doi:10.1021/j100193a062

18. Wyant, J. C. (1982). 3.8 Micron Interferometry For Testing Coated Optics. *Optical Thin Films*. doi:10.1117/12.933297
19. Filmetrics, Inc. (n.d.). Thin Film Thickness Measurement Systems by Filmetrics. Retrieved from https://www.filmetrics.com/
20. Automatic Spray-LBL Machine Based on in-Situ QCM Monitoring. (n.d.). Retrieved from http://pubs.acs.org/doi/abs/10.1021/ma200024w
21. Academicjournals.org. (2018). [online] Available at: http://www.academicjournals.org/article/article1380730068_Oloomi%20et%20al..pdf [Accessed 1 Aug. 2018].
22. Garnett, E., & Yang, P. (2010). Light Trapping in Silicon Nanowire Solar Cells. *Nano Letters, 10*(3), 1082-1087. doi:10.1021/nl100161z
23. Leem, J. W., Yu, J. S., Heo, J., Park, W., Park, J., Cho, W. J., & Kim, D. E. (2014). Nanostructured encapsulation coverglasses with wide-angle broadband antireflection and self-cleaning properties for III–V multi-junction solar cell applications. *Solar Energy Materials and Solar Cells, 120*, 555-560. doi:10.1016/j.solmat.2013.09.038
24. Sheng, X., Liu, J., Kozinsky, I., Agarwal, A. M., Michel, J., & Kimerling, L. C. (2010). Design and Non-Lithographic Fabrication of Light Trapping Structures for Thin Film Silicon Solar Cells. *Advanced Materials, 23*(7), 843-847. doi:10.1002/adma.201003217
25. 4 2C-T-2, 2C-T-7. (2005). *Das Drogentaschenbuch*. doi:10.1055/b-0034-4967
26. Trezzi, D. (2012). *Acta Physica Polonica B, 43*(2), 221. doi:10.5506/aphyspolb.43.221
27. Z, M. S., & N, S. (2015). Analysis of Reflectance and Transmittance Characteristics of Optical Thin Film for Various Film Materials, Thicknesses and Substrates. *Journal of Electrical & Electronic Systems, 04*(03). doi:10.4172/2332-0796.1000160
28. RefractiveIndex.INFO. (n.d.). Retrieved from https://refractiveindex.info/?shelf=main&book=TiO2&page=Siefke
29. RefractiveIndex.INFO. (n.d.). Retrieved from https://refractiveindex.info/?shelf=glass&book=BK7&page=SCHOTT
30. Hassanien, Ahmed & A Akl, Alaa. (2015). Influence of composition on optical and dispersion parameters of thermally evaporated non-crystalline Cd50 S50-xSex thin films. Journal of Alloys and Compounds. 648. 280-290. 10.1016/j.jallcom.2015.06.231.

31. G., A., E., & M., M. (2013, October 08). Structural, Optical Constants and Photoluminescence of ZnO Thin Films Grown by Sol-Gel Spin Coating. Retrieved from https://www.hindawi.com/journals/acmp/2013/234546/
32. Czanderna, A. (1981). Stability of interfaces in solar energy materials. *Solar Energy Materials, 5*(4), 349-377. doi:10.1016/0165-1633(81)90071-x
33. Kalyanasundaram, K. (2010). *Dye-sensitized solar cells*. Lausanne: EPEL Press.